Supporting Information

Thiophene assisted cellular uptake enhancement for highly efficient NIR-II cancer phototheranostics

Yue Zhang[a,#], Jia Yu [a,#], Chunbin Li [a], Jianye Gong [a],Yifan Wu [a], Lina Feng[a], Zihan Chen [a], Renmanduhu Sha [a], Guoyu Jiang[a,*] and Jianguo Wang [a,b,*]

[a]*College of Chemistry and Chemical Engineering, Inner Mongolia Key Laboratory of Fine Organic Synthesis, Inner Mongolia University, Hohhot 010021, P. R. China*
[b]*Institutes of Biomedical Sciences, Inner Mongolia University, Hohhot 010021, P. R. China*

[#] These authors contribute equally to this article.

∗ Corresponding author. e-mail: jiangguoyu@mail.ipc.ac.cn (G. Jiang), wangjg@imu.edu.cn (J. Wang).

Experimental Procedures

Materials

2-(3-cyano-4,5,5-trimethylfuran-2-ylidene)propanedinitrile was purchased from SunaTech. 4-(N,N-Diphenylamino)benzaldehyde, diphenylamine and 2-Bromothiophene were purchased from Adamas. 2,6-dimethyl-γ-pyrone Was purchased from Innochem. Phosphate buffered solution (PBS, pH 7.4) and 2',7'-dichlorodihydrofluorescein diacetate (DCFH-DA) were purchased from Sigma-Aldrich. Thiazolyl blue tetrazolium bromide (MTT) was purchased from Beyotime Biotechnology Co., Ltd. All other chemicals and reagents were purchased from Aladdin and used directly without further purification.

Instruments

^{1}H and ^{13}C NMR spectra were recorded with a Bruker ARX 500 NMR or Bruker ARX 600 NMR spectrometer using tetramethylsilane (TMS) as a reference at room temperature. The high-resolution mass spectra (HRMS) were collected with an LCMS9030 spectrometer. Absorption spectra were measured on a SHIMADZU UV-2600i spectrophotometer. The photoluminescence (PL) spectra were recorded on an FS5 spectrofluorometer. Size distribution was analyzed on a dynamic light scattering (DLS) using an Omni NanoBrook. Particle size and morphology were observed on a FEI Tecnai F20 transmission electron microscope (TEM). Photodynamic and photothermal experiments were implemented by using a 660 nm infrared semiconductor laser (CNIlaser, MDL-XD-660-5W). The temperature change was monitored by a FLIR E8-XT camera (FLIR System). Density functional theory (DFT) calculations were carried out by Gaussian 09 package. The absorbance of each sample was measured using a microplate reader (BioTek) for MTT assay. Cellular uptake assays were assessed by flow cytometry using CytoFLEX (Beckman Coulter). The in vivo NIR-II fluorescence was imaged by the NIR-II fluorescence imaging instrument (Series III 900/1700, Suzhou NIR-Optics Co., Ltd., China) utilizing 900 nm LP filter. The blood biochemistry parameters were collected by the fully automatic biochemical analysis (Chemray 240). Cellular imaging experiments were performed with an inverted fluorescence microscope (Nikon Ti2).

Preparation of nanoparticles

$DSPE\text{-}PEG_{2000}$ (15 mg) and compounds (3 mg) were dissolved into 1.5 mL THF and mixed homogeneously. The mixed solution was added into 15 mL DD water under ultrasonic conditions for 5 min, then poured into the dialysis bag (molecular weight cutoff (MWCO) = 3600). The nanoparticles were obtained by dialysis against deionized water for 24 h until all THF was evaporated. The obtained nanoparticles are concentrated and calibrated for use.

Determination of the relative fluorescence quantum yield (QY) [1, 2]

QY was measured using the NIR fluorescent ICG (QY=2.7%) as the reference.

Fluorescence spectra were tested in water at different absorbances (0.02, 0.04, 0.06, 0.08, and 0.1) upon 660 nm laser excitation. Then, the absorption and emission of NPs in water were measured by an Edinburgh FS5 fluorescence spectrophotometer. The integrated fluorescence spectral area from 670-1300 nm was compared with the corresponding absorbance to fit a linear function, and the relative QY of the sample was calculated according to the following equation:

$$QY_{sample} = QY_{ref} \cdot \frac{slope_{sample}}{slope_{ref}} \cdot (\frac{n_{sample}}{n_{ref}})^2 \quad \text{(a)}$$

where $slope_{\text{sample}}$ and $slope_{\text{ref}}$ are the slopes of the linear functions fitted to the sample and ICG, respectively, and n_{sample} and n_{ref} are the refractive indices of the sample and ICG (water), respectively.

Total ROS detection by DCFH

Dichlorodihydrofluorescein (DCFH) fluorescence intensity was used to detect reactive oxygen species. 50 μL DCFH (40 μM) was mixed with the NPs solution (10 μM) in 2 mL phosphate buffer solution (PBS). Control group were prepared by adding 2 mL PBS in 50 μL DCFH. The mixtures were exposed to 660 nm laser irradiation (400 mW/cm^2), the spectra were tested every ten seconds in a fluorescence spectrometer and the PL intensity at 525 nm was recorded (E_x = 490 nm).

Photothermal properties [3]

The laser power density was first calibrated using an optical power densitometer. The photothermal data of NPs in water (200 μL) at different concentrations (12.5 μM, 25 μM, 50 μM, 100 μM) were measured by irradiation with a 660 nm laser (0.4 W/cm^2) for 5 min, and the curves of photothermal properties with concentrations were obtained. Next, the photothermal data of NPs (100 μM) were measured after irradiation for 5 min at different powers (0.1 W/cm^2, 0.2 W/cm^2, 0.3 W/cm^2, 0.4 W/cm^2) of a 660 nm laser, and the curves of the photothermal properties with irradiation power were obtained.
To evaluate the PCE (η) of NPs, the aqueous solutions of NPs (100 μM) were exposed to 660 nm laser irradiation (0.4 W/cm^2) for 5 min. The laser was then turned off the samples were allowed to cool naturally to room temperature. The photothermal conversion efficiency was calculated according to the following Equation (b):

$$\eta = \frac{hS(T_{Max} - T_{surr}) - Q_{Dis}}{I(1-10^{-A_{660}})} \quad \text{(b)}$$

In equation (b), η is the photothermal conversion efficiency; T_{Max} and T_{Surr} are the equilibrium temperature (ºC) and the ambient temperature of the surrounding (ºC), respectively. Q_{Dis} represents heat dissipated from the laser mediated by the solvent and container. I is 660 nm laser power (mW), and A_{660} is the absorbance of the sample at 660 nm.
The value of hS is obtained from equation (c):

$$\tau_S = \frac{\Sigma_i m_i C_{p,i}}{hS} \quad \text{(c)}$$

In equation (c), hS represents the dimensionless driving force temperature (mW), m is the mass of water (g) and C_p is the heat capacity of water (4.2 J/g), respectively. h is the

heat transfer coefficient, and S is the surface area of the container. τ_s is the sample system time constant (s).
The value of τ_s is obtained from equation (d) and (e):

$$\theta = \frac{T - T_{surr}}{T_{Max} - T_{surr}} \quad \text{(d)}$$

$$t = \tau_s(-\ln\theta) \quad \text{(e)}$$

In equations (d) and (e), T is the solution temperature, and T_{Max} and T_{Surr} are the equilibrium temperature and the ambient temperature of the surroundings, respectively. t is the cooling time point after continuous irradiation for 5 min.

DFT calculations

The molecular geometries were optimized by Gaussian 09 on the calculation level of B3LYP/6-311G(d) under normal convergence criteria. The electron cloud distribution ation and energy calculwere predicted using B3LYP/6-311G(d) based on the optimized structure.

Docking calculation methods

Molecular docking was utilized to predict the binding site residues that interact with ligand based on the X-ray crystal structure (PDB: 3USI). In preparing the protein structures for docking, water was removed and the structures were prepared using the MGL Tools. Ligand was docked into the ligand binding domain using AutoDockTools (version 1.5.6) and Vina. The docking calculation results were analyzed using PyMOL (version 2.5.2).

Cell treatment and cell imaging.

For the imaging, HeLa cells, 4T1 cells, LO2 cells and MCF-7 cells were cultured in DMEM (containing 10% heat-inactivated FBS, 100 mg/mL penicillin and 100 mg/mL streptomycin) at 37 °C in a humidified incubator with 5% CO_2 for 12 h, and then the above cells were treated with four NPs (10 μM) for 12 h. The cells were washed three times with PBS and then imaged using an inverted fluorescence microscopy scanning microscope and cellular uptake was assessed using flow cytometry.

Cellular uptake

Hela cells were cultured in 5% CO_2 for 12 h, 2DSP-PTCF NPs and 2TPA-PTCF NPs (20 μM) were incubated with the cells for varying durations (0 min, 10 min, 20 min, 30 min, 1h, 4h, 8h, 12h). Subsequently, the cells were washed three times with PBS and all groups were observed using inverted fluorescence microscopy.

Quantitative analysis of cell uptake

The 4T1 cells were seeded in DMEM at 37 ºC in a humidified incubator with 5% CO_2 for 12 h, and then 100 μL of cell suspension (~ 5000 cells) was added to each well of a 96-well plate and pre-incubated for 24 h. Subsequently, the 4T1 cells were incubated with four nanoparticles (10 μM) for 12h. The media was then removed, and the cells

were solubilized with Triton X-100 in the presence of ultrasound. Then, the fluorescence intensity of 4T1 cells treated with the four NPs was measured at wavelengths of 750 nm and 850nm using an ELISA Plate Reader (Biotek).

Cell viability

The cells were seeded in DMEM at 37 °C in a humidified incubator with 5% CO_2 for 12 h. Then, the cells in logarithmic growth phase were then harvested and seeded into 96-well plates at a density of 5000 cells/well for another 24 h incubation. The medium was replaced with the fresh medium containing different concentrations of NPs (0 μM, 5 μM, 10 μM, 15 μM, 20 μM, 25 μM, 30 μM). After co-incubating the plate for 20 h in a humidified incubator, the plate was exposed to 660 nm laser irradiation (0.5 W/cm^2) for 10 min and cells without any treatment as a dark group. After further incubation for 4 h, the media was removed and washed with PBS for three times. And then incubate with fresh MTT solution (5 mg/mL in PBS) for 4h, followed by the addition of 100 μL of DMSO to dissolve the formazan crystals. Finally, the absorbance of the products was measured at a wavelength of 490 nm by an ELISA Plate Reader (Biotek). The cells incubated with a culture medium were used as a control. All the experiments were performed in triplicate. The relative cell viability was calculated according to the following formula:

$$Cell\ viability\ (100\%) = \frac{OD_{sample} - OD_{background}}{OD_{control} - OD_{background}} \times 100\%$$

Tumor-bearing mouse model

BALB/c mice (6-8 weeks, average body weight 16-18 g) were purchased from SPF Biotechnology Co., Ltd. (Beijing, China). All animals were cared for in accordance with the guidelines outlined in the Guide for the Care and Use of Laboratory Animals. The procedures were approved by the Institutional Animal Care and Use Committee at the Inner Mongolia University (IMU-2022-mouse-047). All animals were acclimatized to the animal facility for one week before experimentation and housed under pathogen-free conditions, fed under conditions of 25 °C and 55% humidity and allowed free access to standard laboratory water and chow. To establish the xenograft 4T1-tumor-bearing mouse models, 4T1 breast cancer cells (1×10^6) suspended in 100 μL PBS buffer were injected subcutaneously into the right thigh of each mouse. After about 7 days, mice with tumor volumes at about 100 mm^3 were used subsequently. Tumor volumes were measured every day using a caliper and calculated using the following formula:

$$volume = \frac{(tumor\ length) \times (tumor\ width)^2}{2}$$

NIR-II fluorescence imaging

The NIR-II fluorescence images were acquired using the NIR-II fluorescence imaging instrument (Series III 900/1700, Suzhou NIR-Optics Co., Ltd., China). The 4T1-tumor-bearing nude mice were administered with 2DSP-PTCF NPs (400 μM, 150 μL) through

intravenous injection, and NIR-II fluorescence imaging of the tumors was acquired at different post-injection times. After 72 h of injection, mice were euthanized and NIR-II fluorescence images of normal tissues and tumors were collected.

In vivo photothermal therapy and biosafety assessment of NPs

At a tumor volume of approximately 100 mm^3, 4T1 tumor-bearing mice were randomly divided into four groups: PBS, PBS + L, 2DSP-PTCF NPs, and 2DSP-PTCF NPs + L. 100 μL PBS or 100 μL 2DSP-PTCF NPs (500 μM) were directly injected into tumors. For the PBS + L and 2DSP-PTCF NPs + L groups, tumor sites were exposed to 660 nm laser radiation (0.5 W/cm^2) for 10 min after 24 h post injection. Meanwhile, the in vivo photothermal imaging of mice and surface temperature changes of tumors were recorded by an infrared thermal imaging camera (FLIR E8-XT). In the next 15 days, the weight and tumor volume of mice were recorded once a day and calculated as follows: volume = length × $width^2$ / 2. Subsequently, blood from the mice was collected into anticoagulated tubes containing EDTA on the last day, and centrifuged for 15 min to take the supernatant. All plasma samples from the different groups were acquired for kidney and liver function. In the end, the mice were sacrificed by injecting an overdose of narcotics and the major organs (heart, liver, spleen, lung, and kidney) and tumors were collected and imaged using the DSLR camera. Tumors in all groups were collected for antitumor efficacy assessment, and major organs were collected for H&E staining and immunofluorescence staining (TUNEL).

Hemocompatibility test.

Whole blood was collected from healthy mice, centrifuged at 500 g for 10 min to separate the serum and blood cells. The blood cells were then washed thrice with phosphate buffer buffer (PBS). Subsequently, 40 μL of blood cells were treated with varying concentrations of 2DSP-PTCF NPs (0, 5, 10, 15, 20, 25, 30 μM) in polyethylene pipe containing 1 mL of PBS, and incubated for 1 h at 37 ℃. PBS and 0.1% Triton X-100 (Triton) were used as negative control and positive control, respectively. Then, all samples were centrifuged for 10 min, and images were captured. The absorbance of the supernatant was measured at 540 nm. To correct for compound absorbance, a 2DSP-PTCF NPs in PBS solution with the same concentration was used as the blank group. Hemolysis was calculated using the following formula:

$$Hemolysis\ (100\%) = \frac{A_{Blood} - A_{Sample}}{A_{Triton} - A_{PBS}} \times 100\%$$

where A_{Blood} and A_{Sample} represent the absorbance of blood-containing and blood-free PBS solution treated with varying concentrations of 2DSP-PTCF NPs, respectively. A_{Triton} and A_{PBS} denote the absorbance of blood-containing PBS solution treated with and without Triton X-100, respectively.

In vivo pharmacokinetics study

The BALB/c mice were intravenously injected with 2DSP-PTCF NPs. After different time intervals (1/60, 5/60, 10/60, 15/60, 30/60, 1, 2, 3, 6, 9, 12, 24, 36, 48 and 72 h), blood was taken from the tail artery and stored in heparinized tubes. The calibration

curve was obtained by plotting the fluorescence intensity of 2DSP-PTCF NPs versus its concentration. The fluorescence intensity was determined by a VISQUE in vivo smart imaging system (Vieworks Co., Ltd., Korea). Excitation wavelength: 630-680 nm, emission filter: 810-860 nm.

Statistical Analysis

All data were expressed in this article as mean result ± standard deviation (s.d.). All figures shown in this article were obtained from three or more independent experiments with similar results unless specifically mentioned. Statistical significance of differences between groups was tested by SPSS 25 software for samples. A value of $P < 0.05$ was considered significant and was indicated with asterisks: *$P < 0.05$, **$P < 0.01$ and ***$P < 0.001$.

Synthesis and Characterization

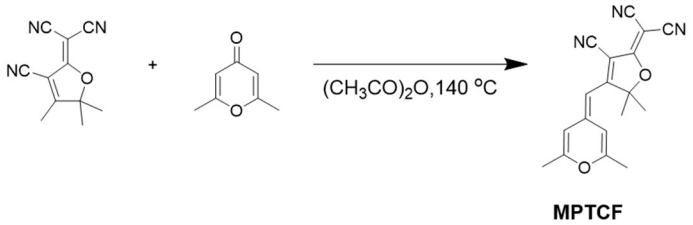

Scheme S1. Synthesis route and molecular structure of MPTCF.

Synthesis of MPTCF: 2-(3-cyano-4,5,5-trimethylfuran-2-ylidene)propanedinitrile (1 g, 1 mmol) and 2,6-dimethyl-γ-pyrone (3.2 g, 5 mmol) were dissolved in 20 mL acetic anhydride under N_2 atmosphere and reacted at 140 ºC for 12 h. After cooling the solution to room temperature, neutralizing by the addition of saturated aq. $NaHCO_3$ solution until bubbles were no longer visible. Then the mixture was extracted with dichloromethane and the organic phase was collected and evaporated under vacuum to obtain the crude product. The crude product was purified by silica gel column chromatography to obtain the target product MPTCF with 45% yield. ^{1}H NMR (500 MHz, $CDCl_3$): δ 6.67 (s, 1H), 6.28 (s, 1H), 5.20 (s, 1H), 2.41 (s, 3H), 2.31 (s, 3H), 1.55 (s, 6H); ^{13}C NMR (126 MHz, $CDCl_3$): δ 178.85, 173.99, 163.74, 162.81, 150.87, 113.81, 113.24, 113.18, 113.04, 111.38, 97.61, 97.03, 87.11, 51.38, 51.26, 20.50, 19.91.

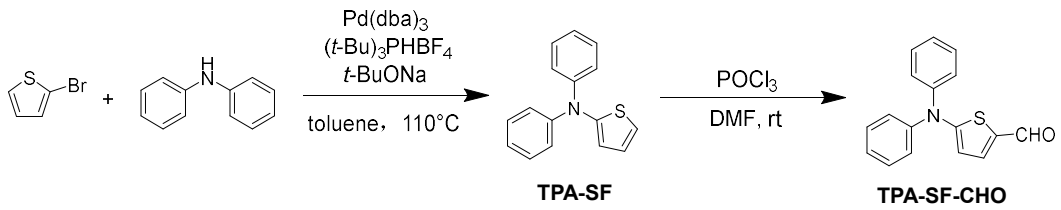

Scheme S2. Synthesis route and molecular structure of TPA-SF-CHO.

Synthesis of TPA-SF-CHO: 2-Bromothiophene (2 g, 1.2 mmol), diphenylamine

(2.157 g, 1 mmol), $Pd(dba)_3$ (280 mg, 0.03 mmol) and $(t\text{-}Bu)_3PHBF_4$ (1.18 g, 1.2 mmol), and ultra-dry toluene (30 mL) were added to a two-neck flask and stirred at room temperature under N_2 atmosphere. Then *t*-BuONa was dissolved with ultra-dry toluene and added into the reaction flask, stirred at room temperature for 30 min, and then heated to 110 ℃ and refluxed for 15 h. After the reaction, the solution was cooled to room temperature and concentrated under vacuum. The compound TPA-SF was then purified by silica gel column chromatography with 45% yield. TPA-SF (2 g, 1 mmol) and dry DMF (10 mL) were added in a two-neck flask equipped under an N_2 atmosphere. $POCl_3$ (1.36 g, 1.1 mmol) was dissolved into dry DMF then added to the flask via syringe and stirred overnight at room temperature. After the reaction, the solution was extracted with dichloromethane and water, and the organic phase was collected and evaporated under vacuum. The compound TPA-SF-CHO was obtained by silica gel column chromatography with a yield of 42%. ^1H NMR (600 MHz, $CDCl_3$): δ 9.61 (s, 1H), 7.46 (d, J = 4.3 Hz, 1H), 7.37 (t, J = 8.2 Hz, 4H), 7.28 (d, J = 7.6 Hz, 4H), 7.22 (t, J = 7.4 Hz, 2H), 6.39 (d, J = 4.3 Hz, 1H).

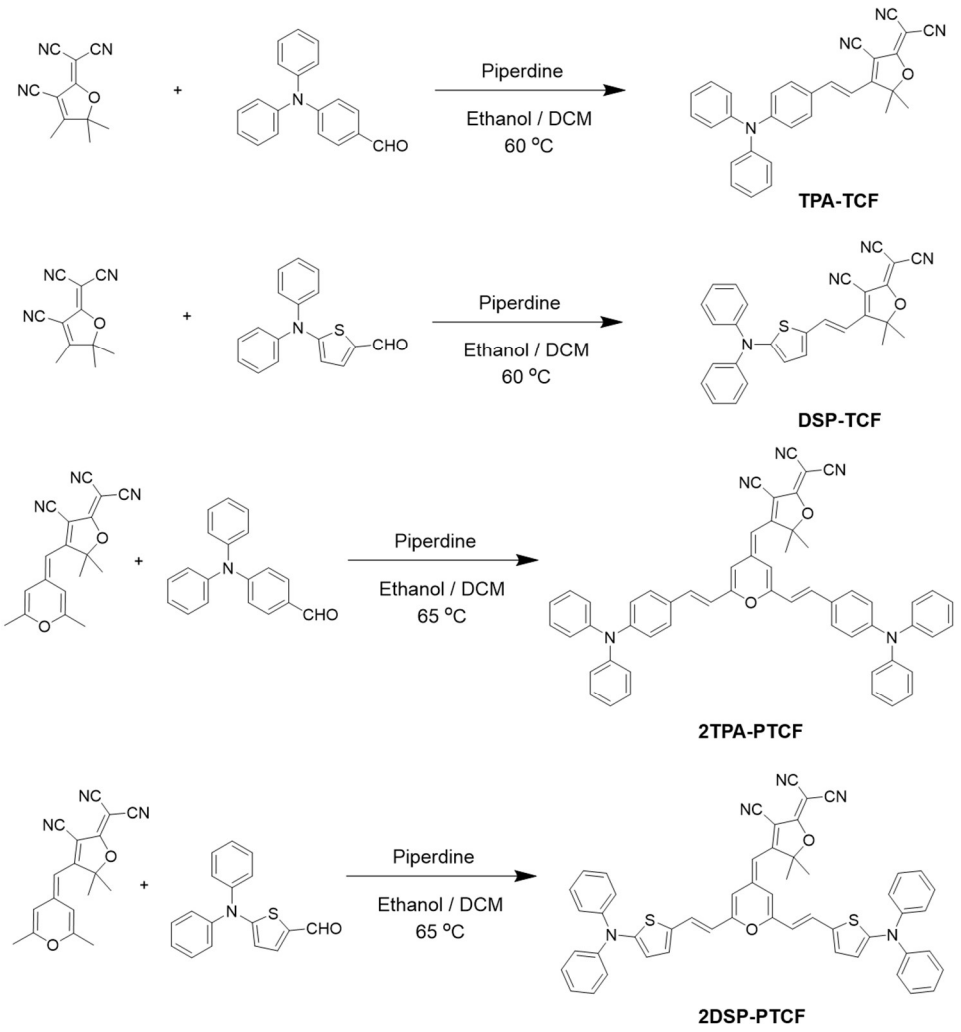

Scheme S3. Synthesis route and molecular structure of TPA-TCF, DSP-TCF, 2TPA-PTCF, 2DSP-PTCF.

Synthesis of TPA-TCF: 2-(3-Cyano-4,5,5-trimethylfuran-2-ylidene)propanedinitrile (200 mg, 1 mmol) and 4-formyltriphenylamine (274.6 mg, 1 mmol) were dissolved in 18 mL of ethanol/dichloromethane (5:1, *v/v*). A small amount of piperidine was added dropwise to the solution and the mixture was refluxed overnight at 60 ºC. The solution was cooled to room temperature and concentrated in vacuum to remove ethanol/dichloromethane, then purified by silica gel column chromatography to give TPA-TCF in 33% yield. ^{1}H NMR (500 MHz, $CDCl_3$): δ 7.58 (d, *J* = 16.1 Hz, 1H), 7.46 (d, *J* = 8.6 Hz, 2H), 7.36 (t, *J* = 7.6 Hz, 4H), 7.22 - 7.17 (m, 6H), 6.98 (d, *J* = 8.6 Hz, 2H), 6.82 (d, *J* = 16.0 Hz, 1H), 1.76 (s, 6H); ^{13}C NMR (151 MHz, $CDCl_3$): δ 175.77, 173.91, 152.52, 147.18, 145.67, 131.07, 129.84, 126.35, 125.91, 125.62, 119.89, 112.13, 111.33, 111.17, 110.84, 97.08, 96.79, 56.25, 26.63. HRMS (MALDI-TOF): m/z: $[M+Na]^+$ calcd for $C_{30}H_{22}N_4NaO$: 477.1691; found: 477.1685.

Synthesis of DSP-TCF: The synthetic route was similar to **TPA-TCF** except for the change of starting materials (29%). ^{1}H NMR (500 MHz, $CDCl_3$): δ 7.79 (d, *J* = 15.2 Hz, 1H), 7.44 (t, *J* = 8.0 Hz, 4H), 7.34 - 7.32 (m, 6H), 7.29 (d, *J* = 4.4 Hz, 1H), 6.40 (d, *J* = 4.4 Hz, 1H), 6.05 (d, *J* = 15.1 Hz, 1H), 1.65 (s, 6H); ^{13}C NMR (151 MHz, $CDCl_3$): δ 176.44, 172.83, 165.38, 145.16, 140.45, 140.26, 130.18, 127.74, 127.43, 125.80, 113.64, 112.98, 112.18, 112.03, 107.07, 96.21, 53.62, 26.61. HRMS (MALDI-TOF): m/z: $[M+Na]^+$ calcd for $C_{28}H_{20}N_4NaOS$: 483.1256; found: 483.1254.

Synthesis of 2TPA-PTCF: MPTCF (500 mg, 1 mmol) and 4-formyltriphenylamine (1139 mg, 2 mmol) are dissolved in 24 mL of ethanol/dichloromethane (5:1, *v/v*). A small amount of piperidine is added dropwise to the solution and the mixture was refluxed overnight at 65ºC. The solution was cooled to room temperature and concentrated in vacuum to remove ethanol/dichloromethane, then purified by silica gel column chromatography to give 2TPA-PTCF in 29% yield. ^{1}H NMR (600 MHz, DMSO-d_6): δ 7.73 (d, *J* = 16.0 Hz, 2H), 7.69 (d, *J* = 8.4 Hz, 4H), 7.38 (t, *J* = 7.7 Hz, 8H), 7.16 (t, *J* = 7.5 Hz, 4H), 7.12 (d, *J* = 7.9 Hz, 8H), 7.06 (d, *J* = 16.0 Hz, 2H), 6.95 (d , *J* = 8.4 Hz, 4H), 6.94 (s, 2H), 5.86 (s, 1H), 1.60 (s, 6H); ^{13}C NMR (151 MHz, $CDCl_3$): δ 178.80, 171.52, 159.50, 150.33, 150.10, 146.75, 137.34, 129.60, 129.24, 127.74, 125.62, 124.36, 121.55, 116.26, 114.11, 113.86, 113.42, 99.48, 96.44, 85.84, 50.83, 26.72. HRMS (MALDI-TOF): m/z: $[M+H]^+$ calcd for $C_{56}H_{42}N_5O_2$: 816.3339; found: 816.3339.

Synthesis of 2DSP-PTCF: The synthetic route was similar to **2TPA-PTCF** except for the change of starting materials (21%). ^{1}H NMR (600 MHz, DMSO-d_6): δ 7.84 (d, *J* = 15.6 Hz, 2H), 7.43 (t, *J* = 7.7 Hz, 8H), 7.36 (d, *J* = 4.1 Hz, 2H), 7.28 (d, *J* = 8.0 Hz, 8H), 7.24 (t, *J* = 7.5 Hz, 4H), 6.81 (s, 2H), 6.53 (d, *J* = 15.6 Hz, 2H), 6.45 (d, *J* = 4.1 Hz, 2H), 5.68 (s, 1H), 1.55 (s, 6H). ^{13}C NMR (151 MHz, $CDCl_3$): δ 178.92, 170.35, 159.37, 157.61, 150.24, 146.55, 132.96, 131.28, 130.22, 129.70, 125.83, 125.37, 124.76, 115.21, 114.60, 114.39, 113.96, 113.40, 99.17, 96.10, 83.91, 49.51, 26.80. HRMS (MALDI-TOF): m/z: $[M+H]^+$ calcd for $C_{52}H_{38}N_5O_2S_2$: 828.2467; found: 828.2454.

Supplementary Figures

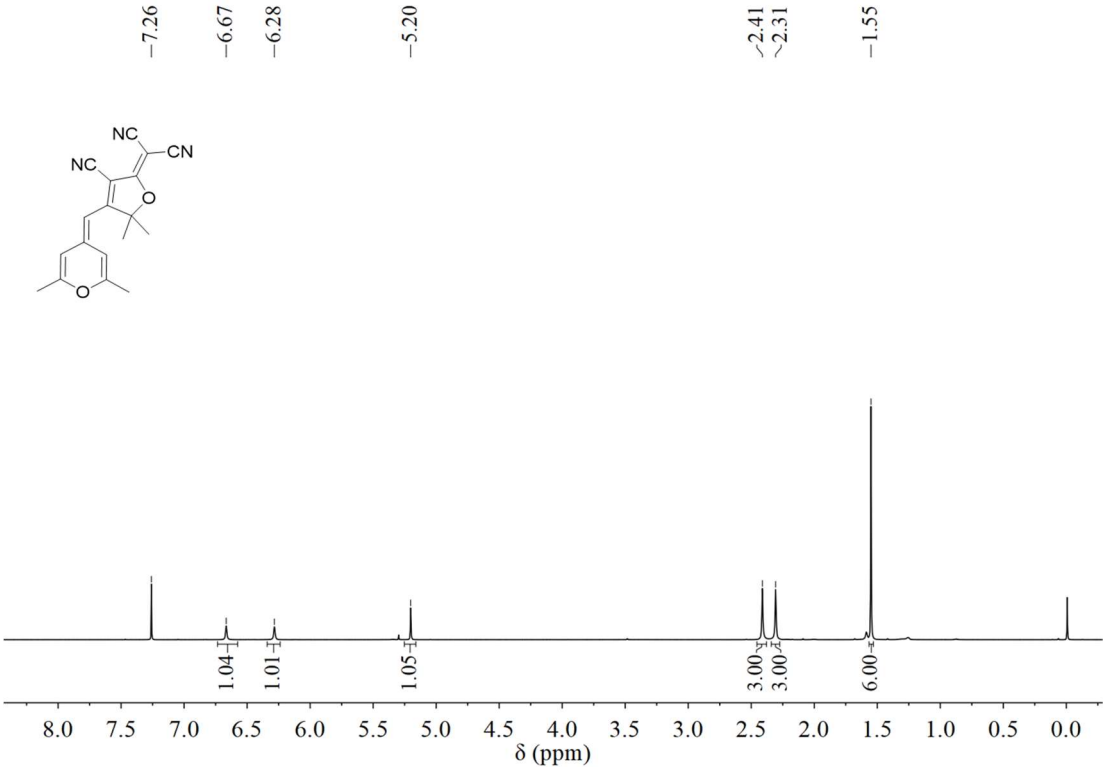

Figure S1. ^{1}H NMR spectrum of compound MPTCF in $CDCl_3$.

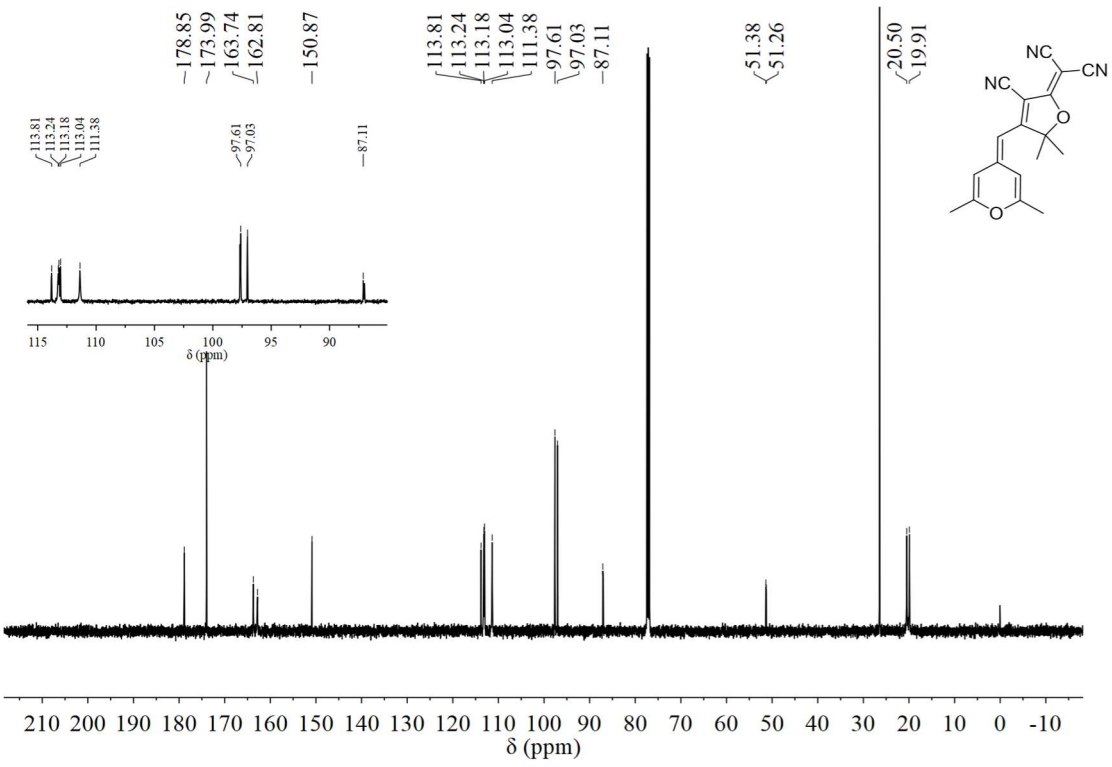

Figure S2. ^{13}C NMR spectrum of compound MPTCF in $CDCl_3$.

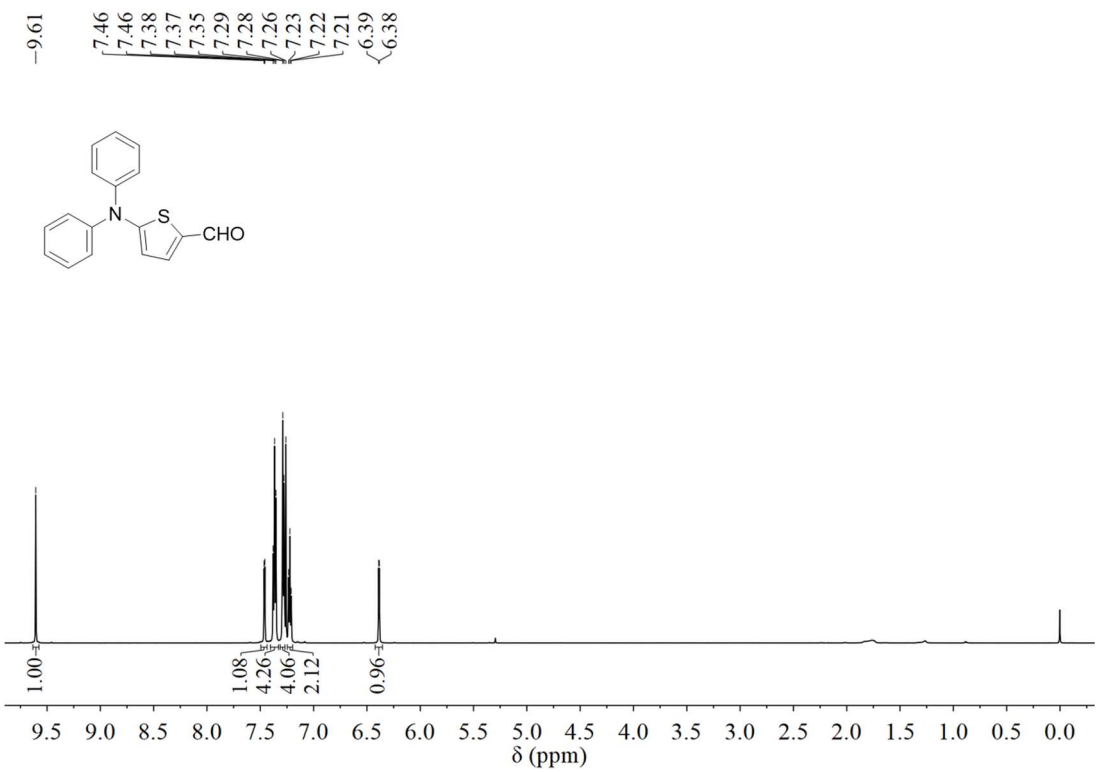

Figure S3. ^{1}H NMR spectrum of compound TPA-SF-CHO in $CDCl_3$.

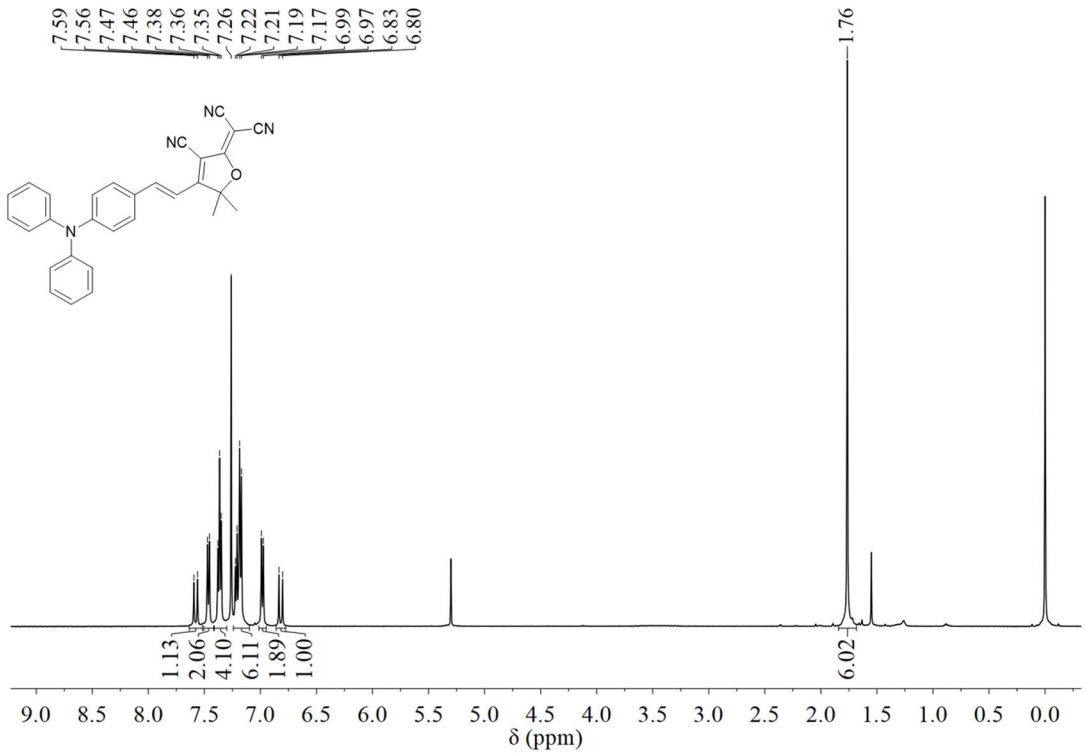

Figure S4. ^{1}H NMR spectrum of compound TPA-TCF in $CDCl_3$.

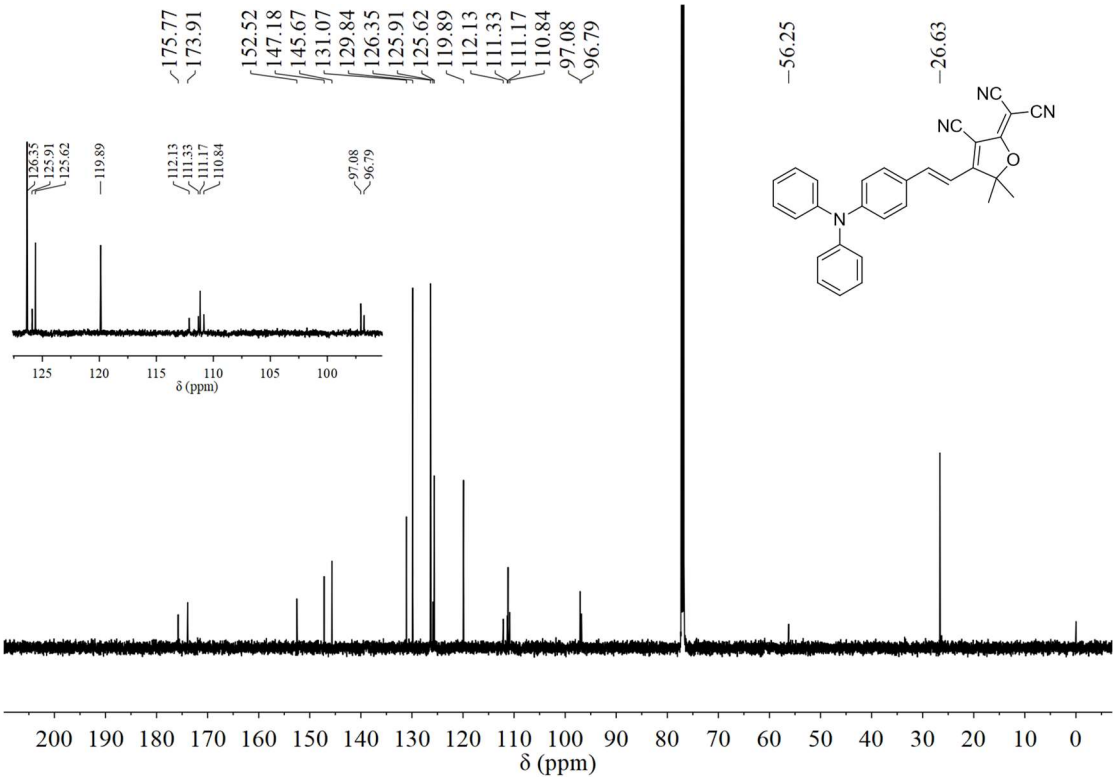

Figure S5. ^{13}C NMR spectrum of compound TPA-TCF in $CDCl_3$.

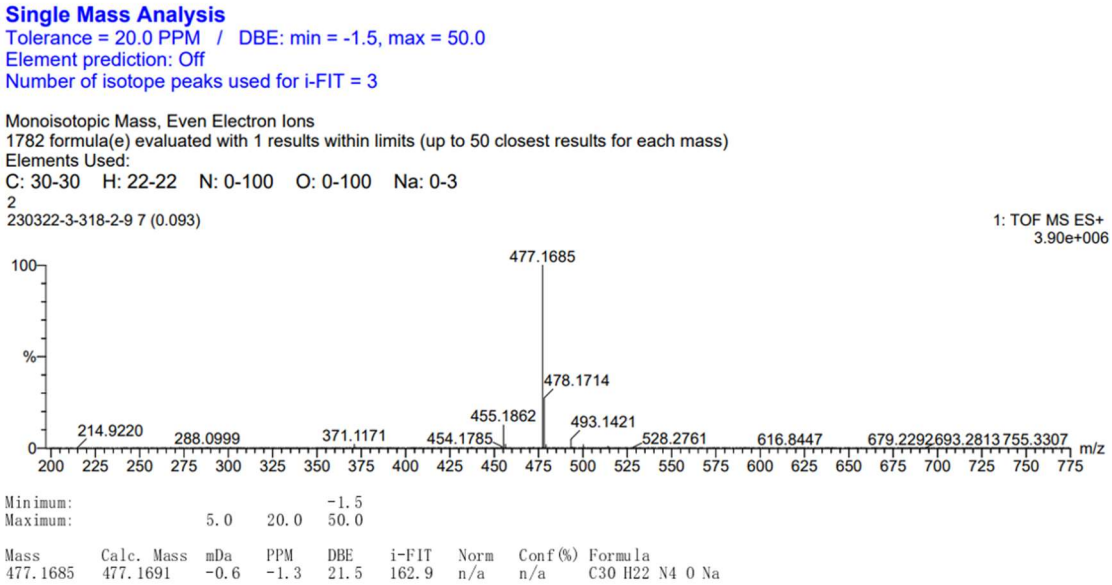

Figure S6. HRMS spectrum of TPA-TCF.

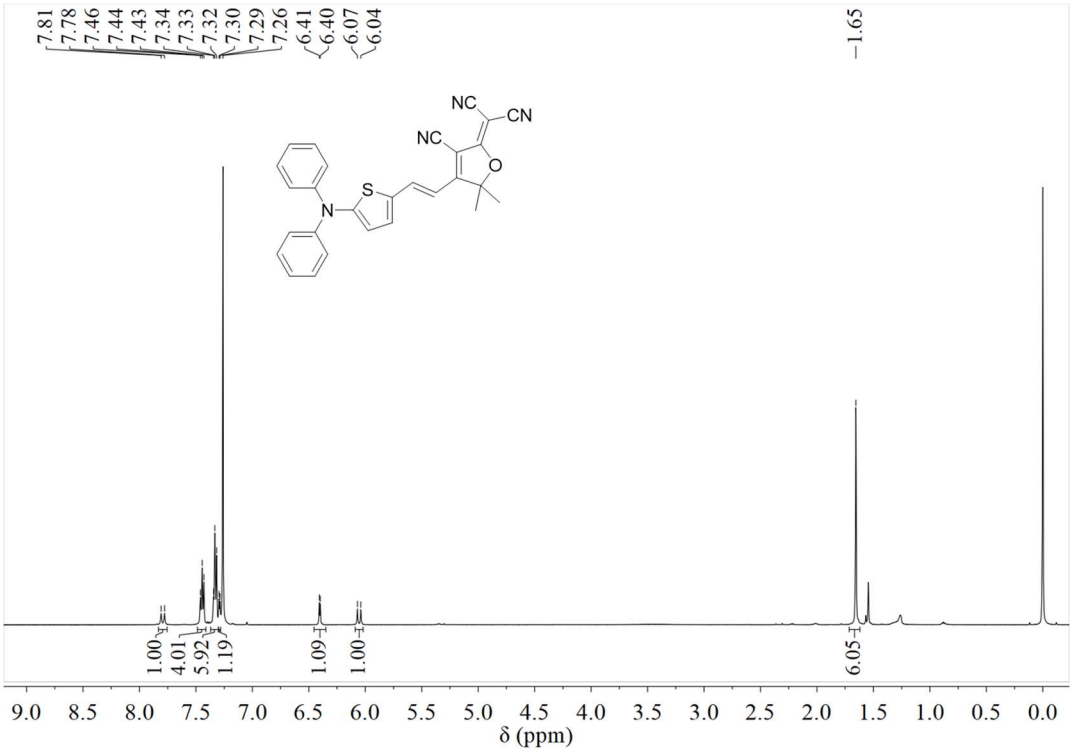

Figure S7. ^{1}H NMR spectrum of compound DSP-TCF in $CDCl_3$.

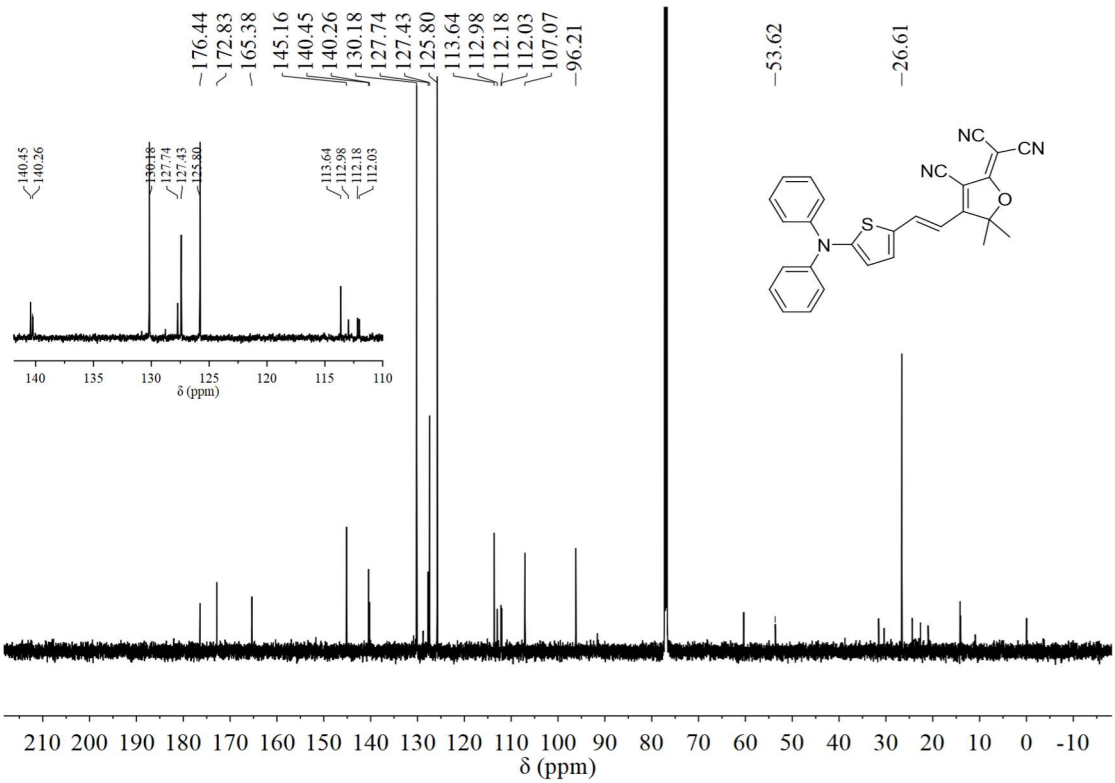

Figure S8. ^{13}C NMR spectrum of compound DSP-TCF in $CDCl_3$.

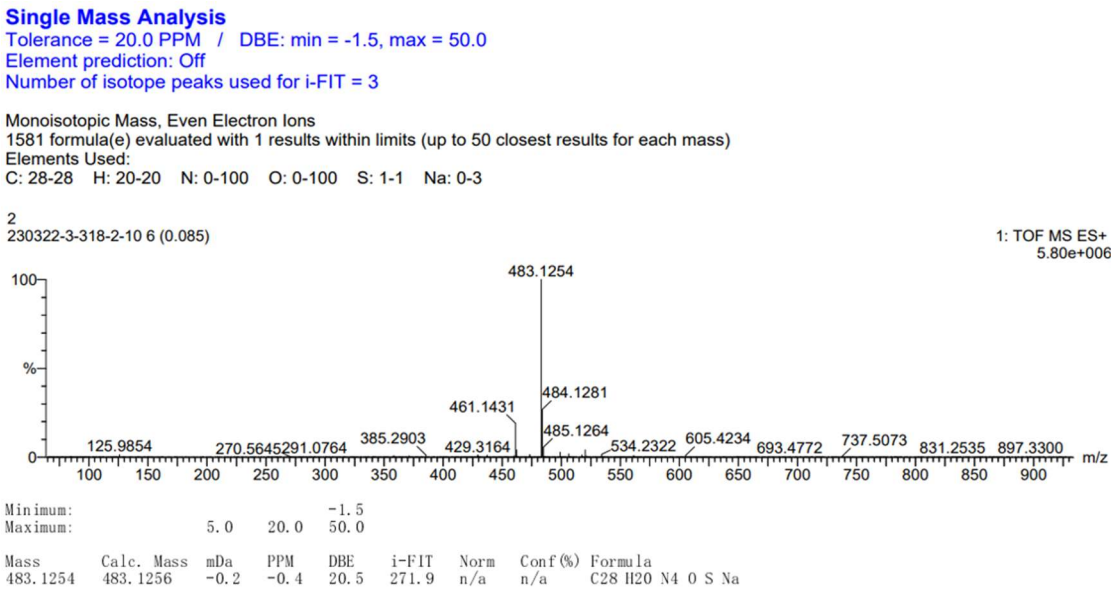

Figure S9. HRMS spectrum of DSP-TCF.

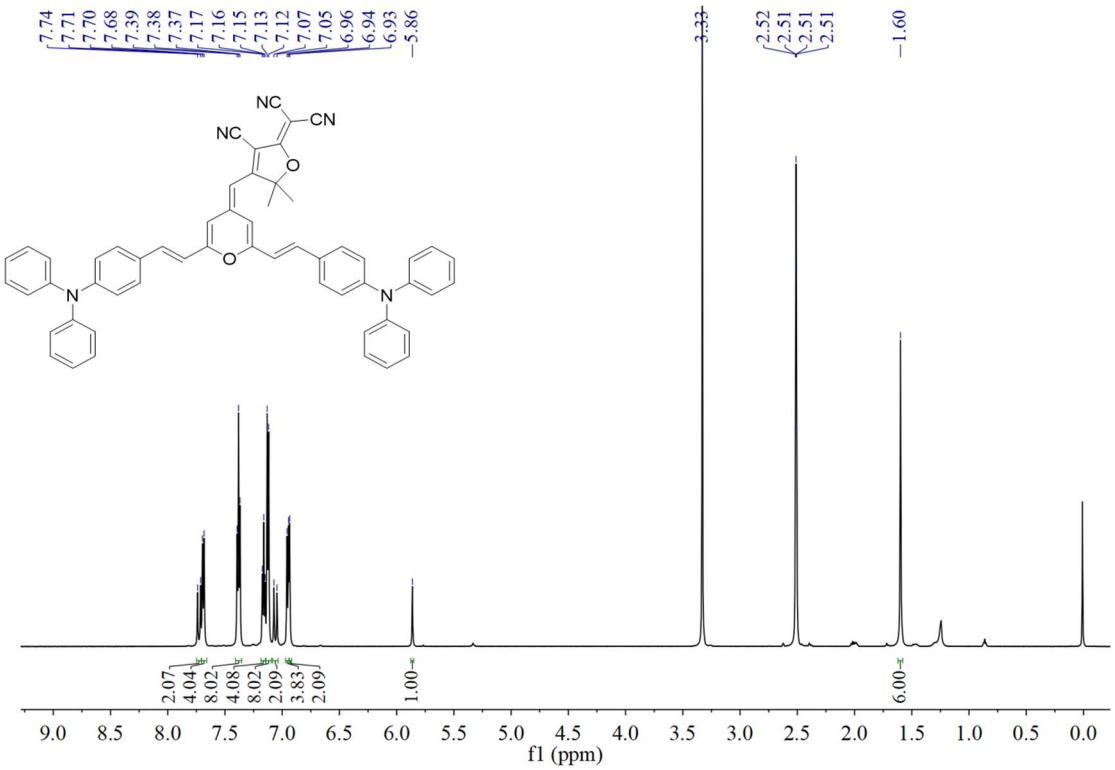

Figure S10. ^{1}H NMR spectrum of compound 2TPA-PTCF in DMSO-d_6.

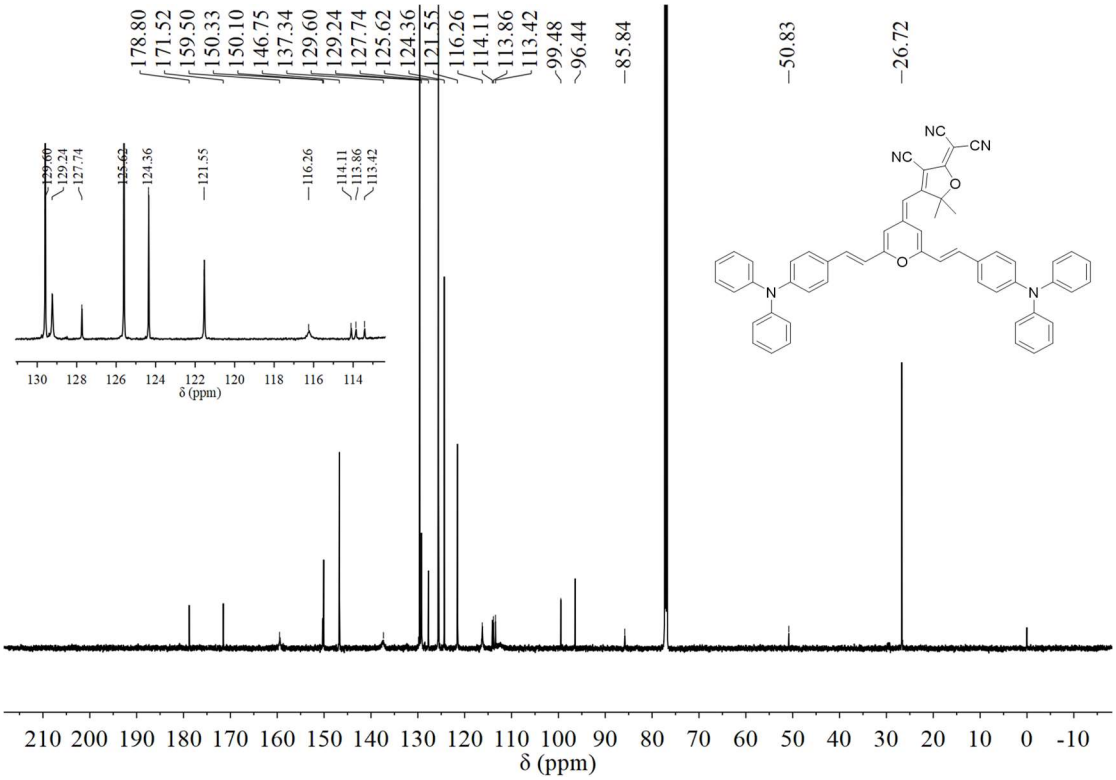

Figure S11. ^{13}C NMR spectrum of compound 2TPA-PTCF in $CDCl_3$.

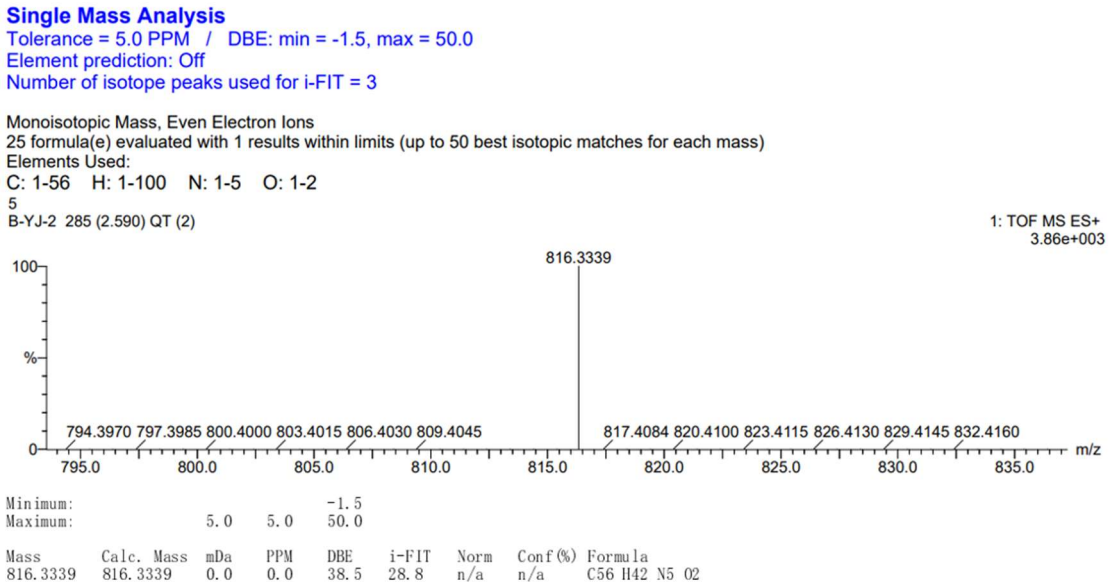

Figure S12. HRMS spectrum of 2TPA-PTCF.

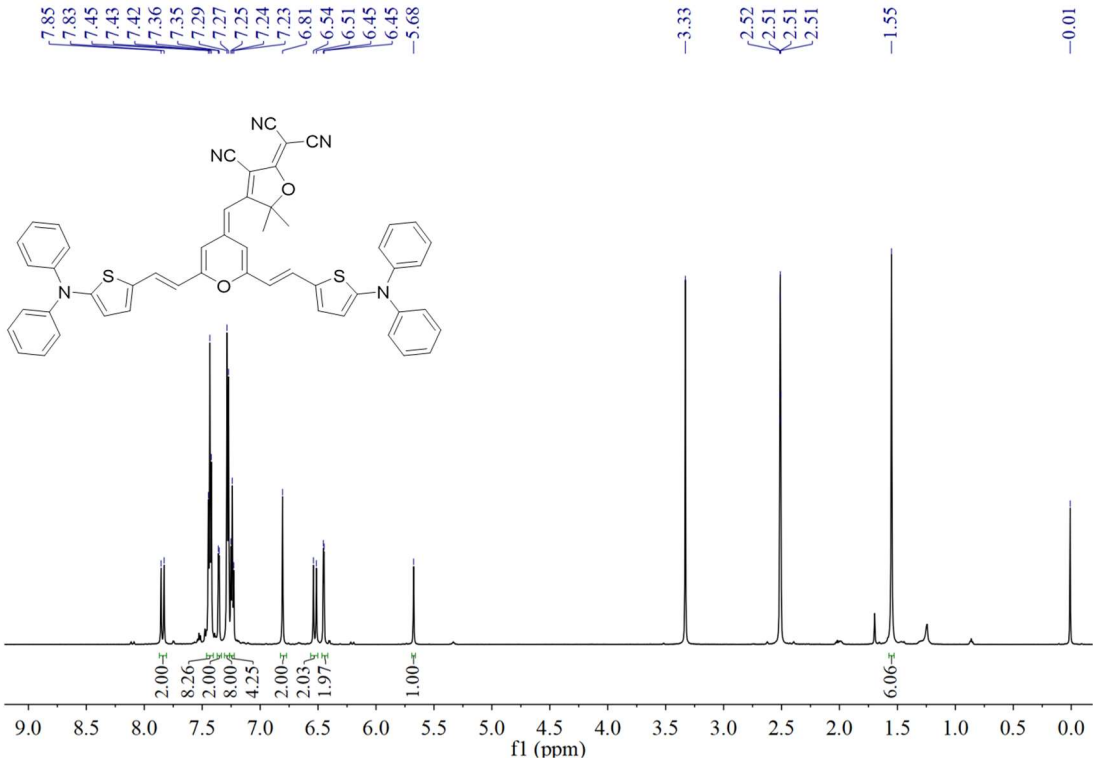

Figure S13. ^{1}H NMR spectrum of compound 2DSP-PTCF in DMSO-d_6.

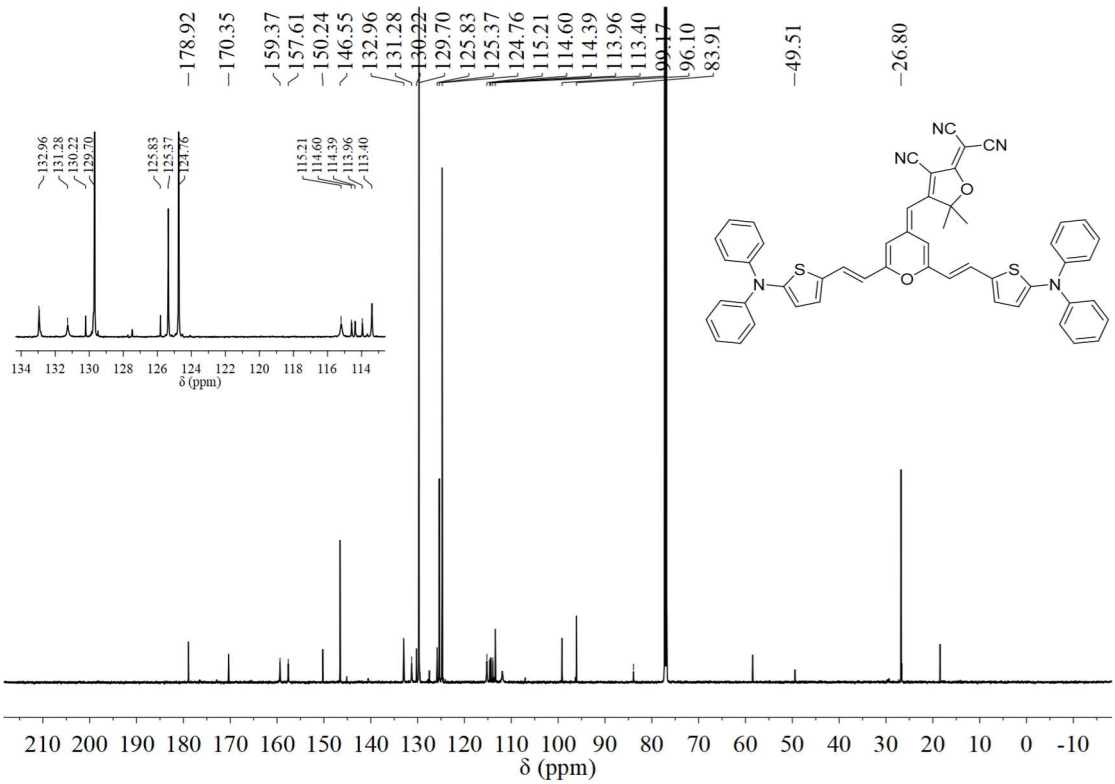

Figure S14. ^{13}C NMR spectrum of compound 2DSP-PTCF in $CDCl_3$.

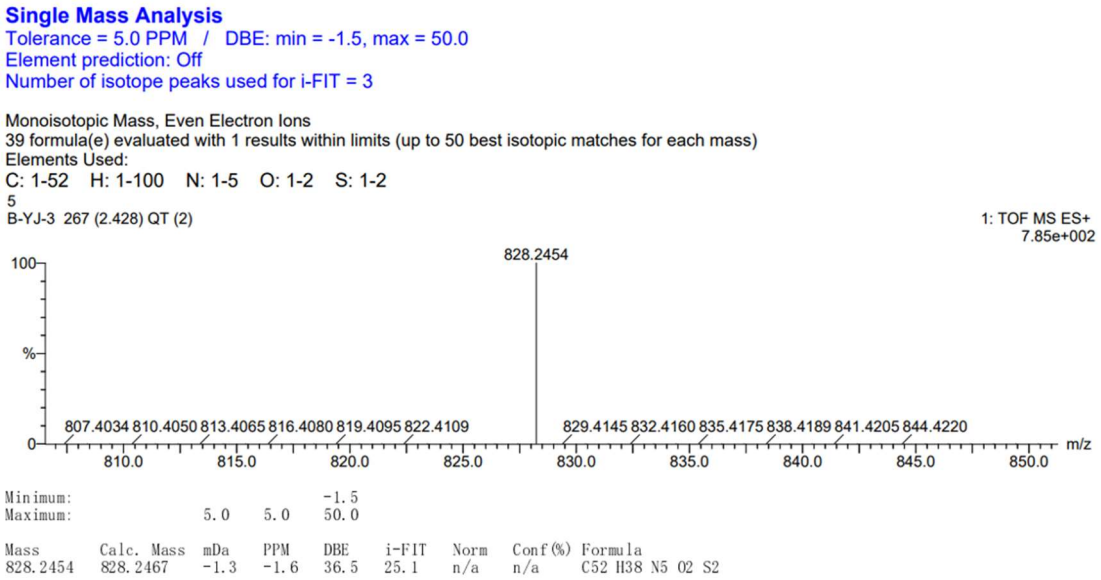

Figure S15. HRMS spectrum of 2DSP-PTCF.

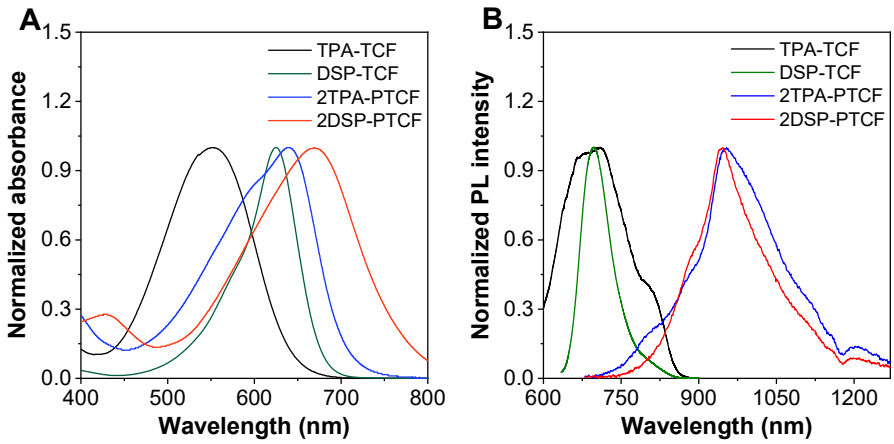

Figure S16. Normalized absorption and fluorescence spectra of the four compounds TPA-TCF, DSP-TCF, 2TPA-PTCF and 2DSP-PTCF in DMSO solution.

Table S1. Photophysical properties of the four compounds.

	Absorbance (nm)		Emission (nm)		Stokes shift (nm)		Molar extinction coefficient ($L\ mol^{-1}\ cm^{-1}$)		CLog P
	In DMSO	In NPs	In DMSO	In NPs	In DMSO	In NPs	In DMSO	In NPs	
TPA-TCF	552	500	704	753	152	253	2.82×10^4	2.66×10^4	5.8
DSP-TCF	626	595	700	745	74	150	5.07×10^4	5.17×10^4	5.6
2TPA-PTCF	639	628	957	944	318	316	9.35×10^4	9.4×10^4	11.7
2DSP-PTCF	667	699	945	940	278	241	1.14×10^5	1.15×10^5	11.2

Table S2. The single crystal X-ray crystallographic data of 2TPA-PTCF and 2DSP-PTCF.

Name	2TPA-PTCF	2DSP-PTCF
Empirical formula	$C_{56}H_{41}N_5O_2$	$C_{52}H_{37}N_5O_2S_2$
Formula weight	815.94	827.98
Temperature (K)	293.00(2)	193.00(2)
Wavelength (Å)	1.54184	0.71073
Crystal system	triclinic	triclinic
Space group	P-1	P-1
a (Å)	10.17742(9)	11.5451(4)
b (Å)	14.91873(16)	13.6561(5)
c (Å)	17.25327(19)	16.0395(6)
α (°)	67.1553(10)	103.1030(10)
β (°)	86.4455(8)	101.6110(10)
γ (°)	80.1926(8)	109.4680(10)
Volume (Å^3)	2378.85(4)	2214.12(14)
Z	2	2
ρ_{calc}g/cm^3	1.139	1.242
μ/mm^{-1}	0.549	0.167
F(000)	856.0	864.0
Crystal size/mm^3	0.15 × 0.12 × 0.1	0.13 × 0.12 × 0.1
2Θ range for data collection (°)	5.558 to 153.066	3.578 to 56.514
Index ranges	-9 ≤ h ≤ 12, -18 ≤ k ≤ 18, -21 ≤ l ≤ 21	-15 ≤ h ≤ 15, -18 ≤ k ≤ 18, -21 ≤ l ≤ 15
Reflections collected	31645	22873
Independent reflections	9674 [R_{int} = 0.0236, R_{sigma} = 0.0239]	10890 [R_{int} = 0.0457, R_{sigma} = 0.0704]
Data/restraints/parameters	9674/0/570	10890/0/552
Goodness-of-fit on F^2	1.081	1.043
Final R indexes [I>=2σ (I)]	R_1 = 0.0417, wR_2 = 0.1149	R_1 = 0.0487, wR_2 = 0.1144
Final R indexes [all data]	R_1 = 0.0464, wR_2 = 0.1184	R_1 = 0.0762, wR_2 = 0.1285
Largest diff. peak/hole / e Å^{-3}	0.13/-0.23	0.32/-0.32
CCDC Number	2341290	2341291

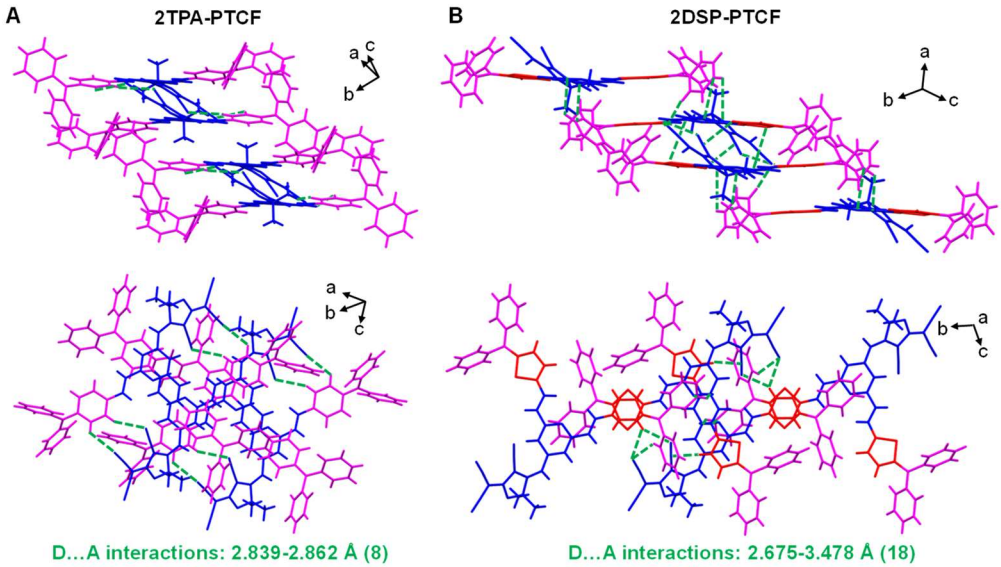

Figure S17. Molecular packing mode and intermolecular interactions of (A) 2TPA-PTCF and (B) 2DSP-PTCF.

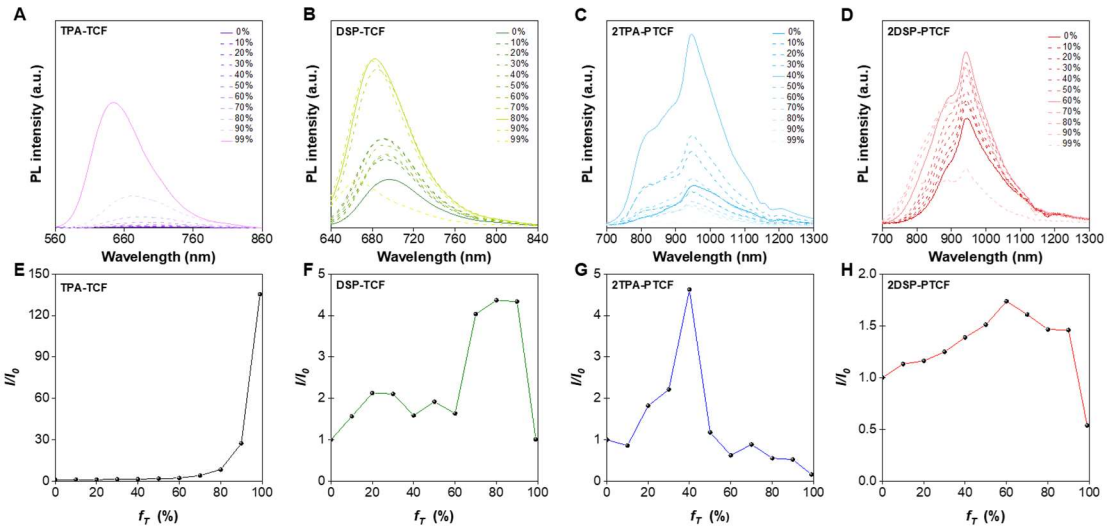

Figure S18. Fluorescence spectra of the four compounds in DMSO/toluene mixtures with different f_T: (A) TPA-TCF; (B) DSP-TCF; (C) 2TPA-PTCF and (D) 2DSP-PTCF; The fluorescence intensity variations with f_T at the maximum emission wavelength of (E) TPA-TCF (E_m=704 nm); (F) DSP-TCF (E_m=700 nm); (G) 2TPA-PTCF (E_m=957 nm) and (H) 2DSP-PTCF (E_m=945 nm).

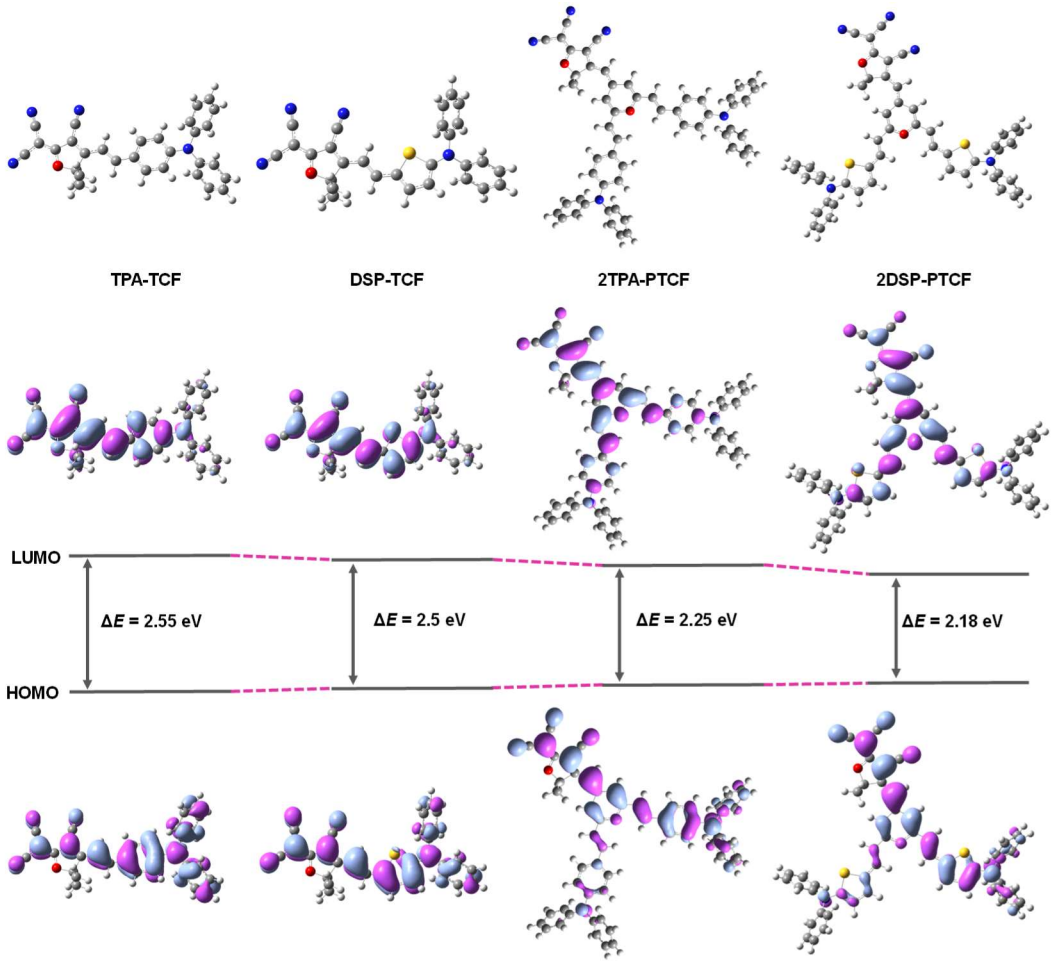

Figure S19. The HOMO and LUMO distributions of the four compounds.

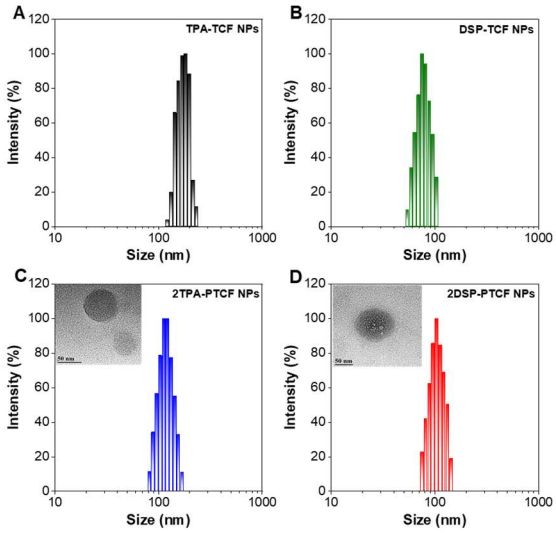

Figure S20. TEM image and DLS results of the (A) TPA-TCF NPs; (B) DSP-TCF NPs; (C) 2TPA-PTCF NPs; (D) 2DSP-PTCF NPs. The inset showed the TEM images of 2TPA-PTCF NPs and 2DSP-PTCF NPs. Scale bar indicates 50 nm.

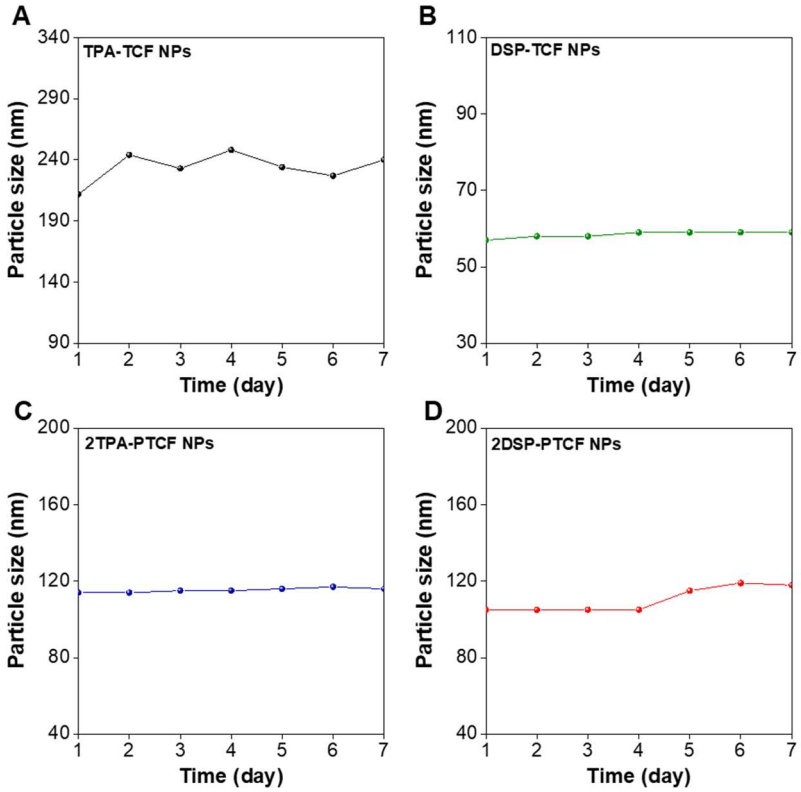

Figure S21. Size changes of four NPs in PBS solution within 7 days: (A) TPA-TCF NPs; (B) DSP-TCF NPs; (C) 2TPA-PTCF NPs and (D) 2DSP-PTCF NPs.

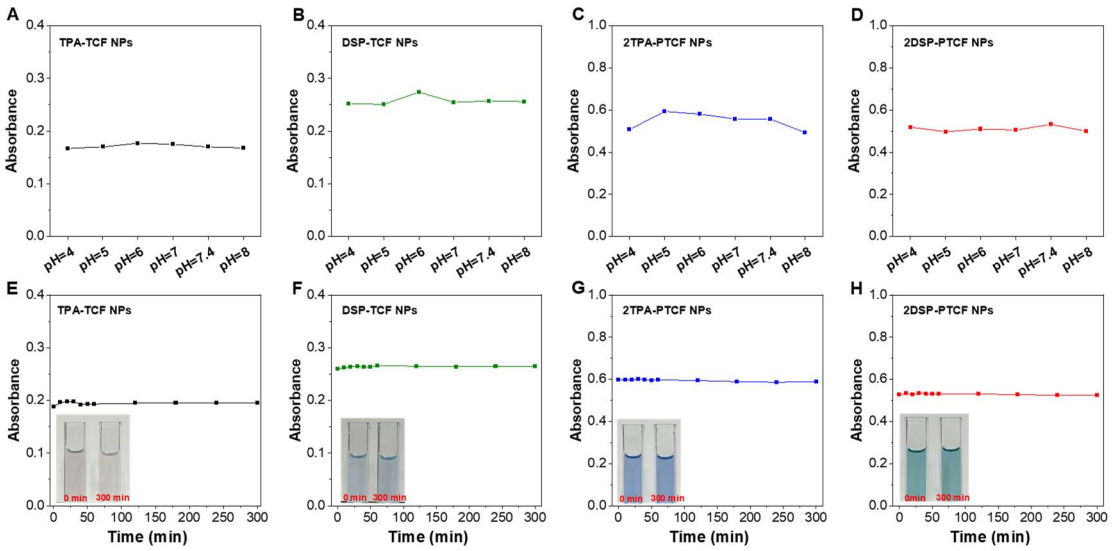

Figure S22. The maximum absorbance intensity of (A) TPA-TCF NPs (@500 nm), (B) DSP-TCF NPs (@595 nm), (C) 2TPA-PTCF NPs (@628 nm) and (D) 2DSP-PTCF NPs (@699 nm) in different pH value solution. The maximum absorbance intensity of (E) TPA-TCF NPs (@500 nm), (F) DSP-TCF NPs (@595 nm), (G) 2TPA-PTCF NPs (@628 nm) and (H) 2DSP-PTCF NPs (@699 nm) in fetal bovine serum (10% FBS) at different storage time. The insert shows the color of the four NPs in 10% FBS at 0 min and 300 min.

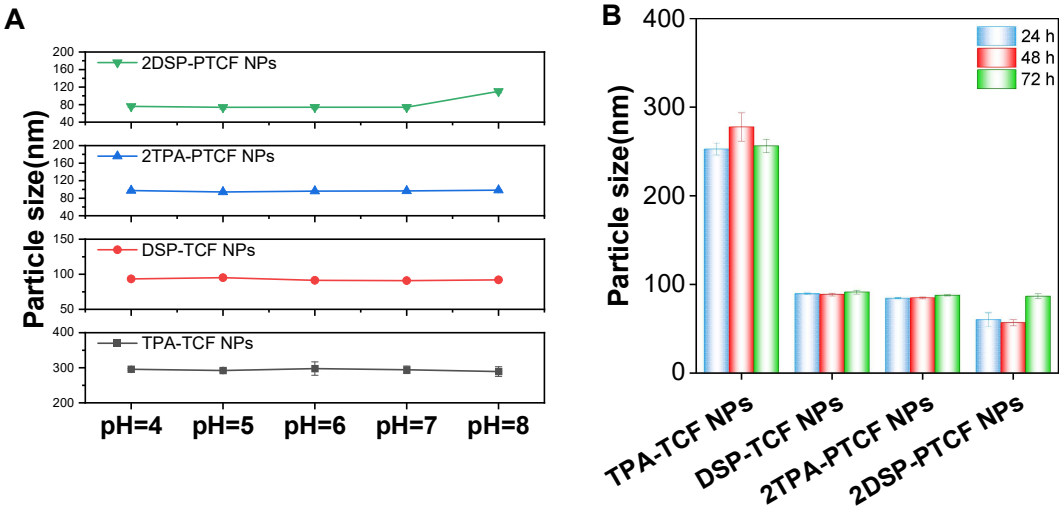

Figure S23. Size changes of four NPs in different pH value solutions (A) and FBS (10%) within 72 h (B).

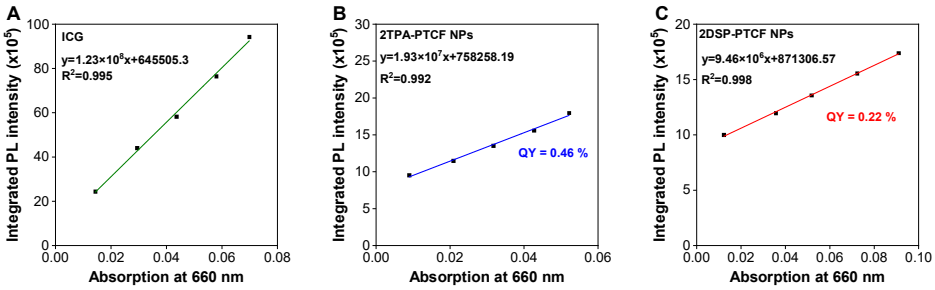

Figure S24. Relative QY with ICG as the reference: (A) ICG; (B) 2TPA-PTCF NPs; (C) 2DSP-PTCF NPs.

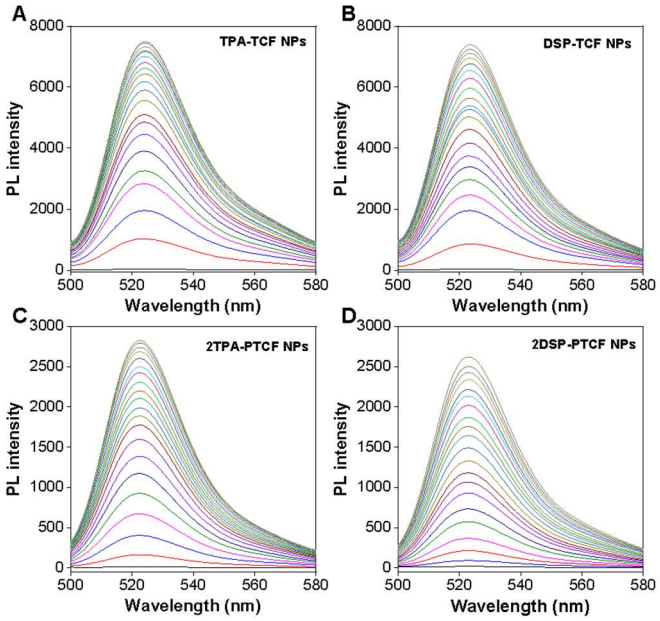

Figure S25. DCFH-DA as the capturing agent to test the total ROS production capacity of the four NPs: (A) TPA-TCF NPs; (B) DSP-TCF NPs; (C) 2TPA-PTCF NPs and (D) 2DSP-PTCF NPs.

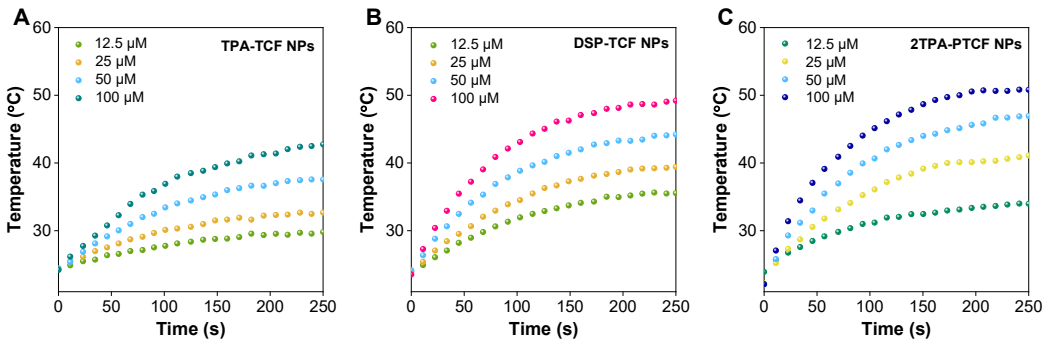

Figure S26. Temperature variation of the NPs at different concentrations under 660 nm laser irradiation (400 mW/cm^2). (A) TPA-TCF NPs; (B) DSP-TCF NPs; (C) 2TPA-PTCF NPs.

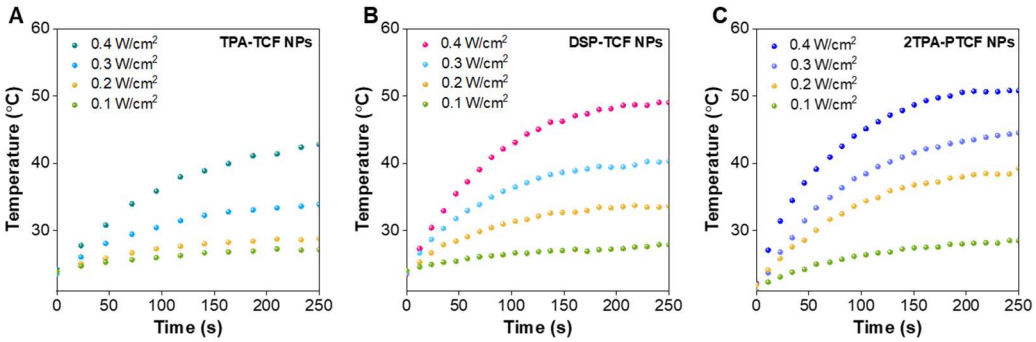

Figure S27. Temperature variation of the NPs under different power of 660 nm laser irradiation. (A) TPA-TCF NPs; (B) DSP-TCF NPs; (C) 2TPA-PTCF NPs. (100 μM).

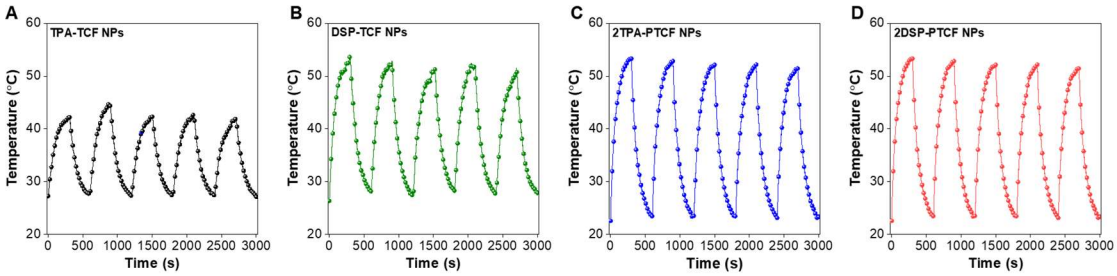

Figure S28. Temperature changes of the four NPs under 5 times of 660 nm laser (400 mW/cm^2) on/off cycle. (A) TPA-TCF NPs; (B) DSP-TCF NPs; (C) 2TPA-PTCF NPs; (D) 2DSP-PTCF NPs. The concentration of the NPs is 100 μM.

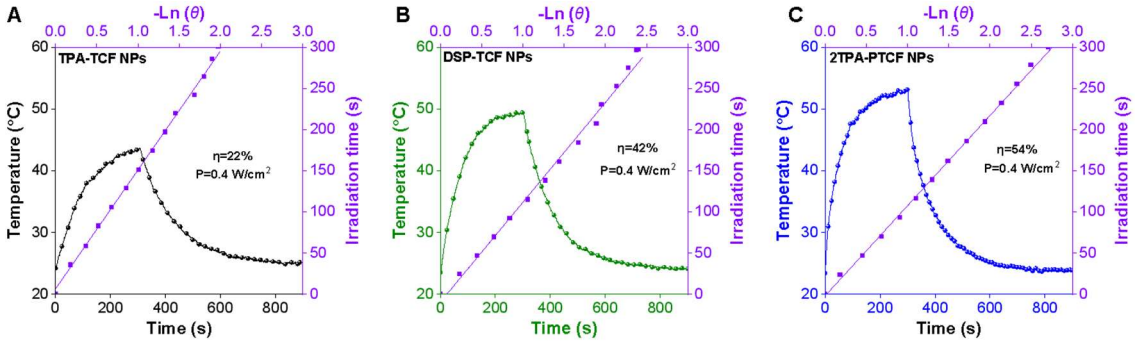

Figure S29. Temperature-increasing/decreasing curve and cooling time vs-ln(θ) plot (θ: temperature driving force). (A) TPA-TCF NPs; (B) DSP-TCF NPs; (C) 2TPA-PTCF NPs. The concentration of the NPs is 100 μM.

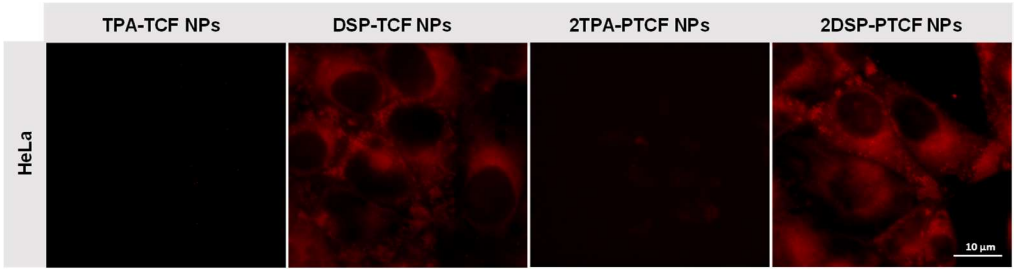

Figure S30. Fluorescence imaging results of the four NPs (10 μM) in HeLa cells after 12 h incubation.

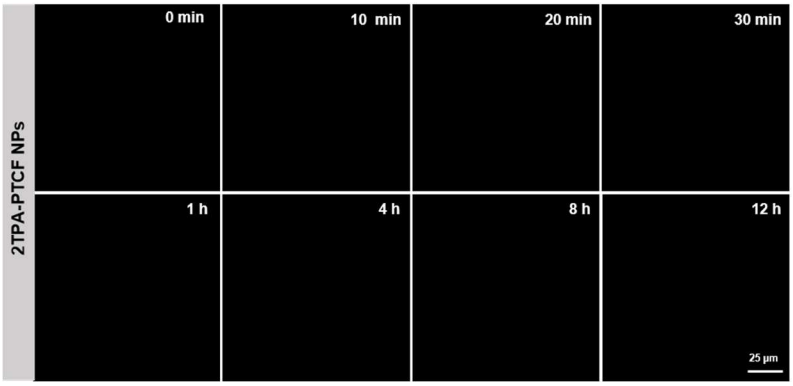

Figure S31. Fluorescence imaging results of 2TPA-PTCF NPs (20 μM) inside HeLa cells after different incubation times.

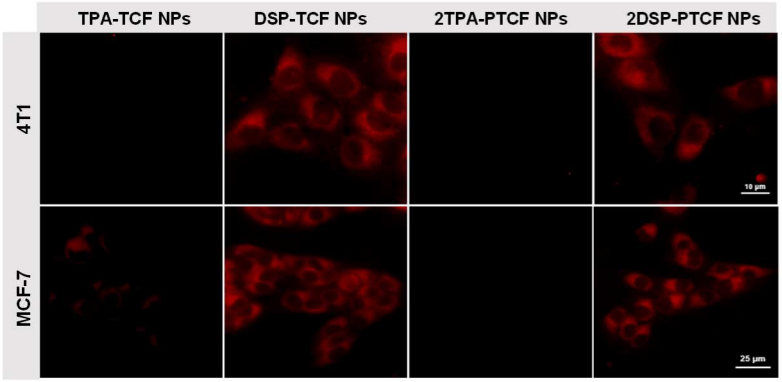

Figure S32. Fluorescence imaging results of the four NPs (10 μM) in 4T1 and MCF-7 cells after 12 h incubation.

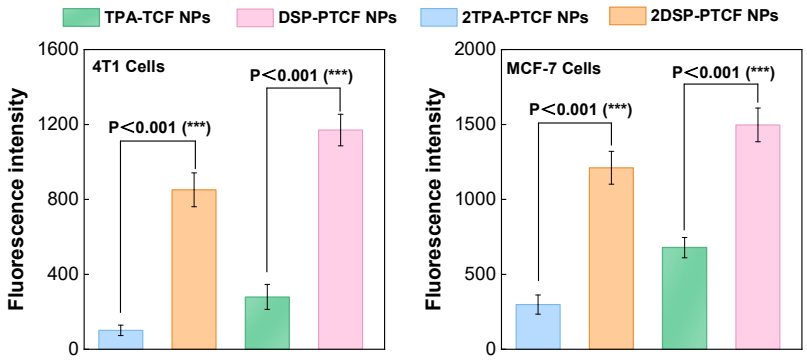

Figure S33. Fluorescence intensity analysis of 4T1 and MCF-7 cells incubated with NPs. (n = 3)

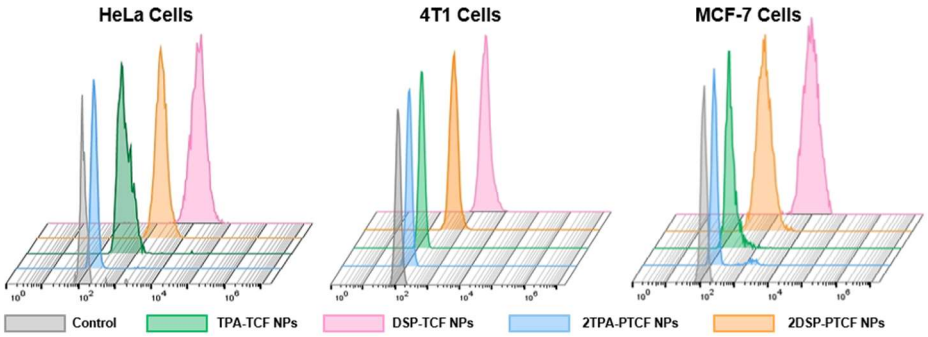

Figure S34. Flow cytometry analysis of cellular uptake levels of different cell after treatment with the four NPs (10 μM) for 12 h.

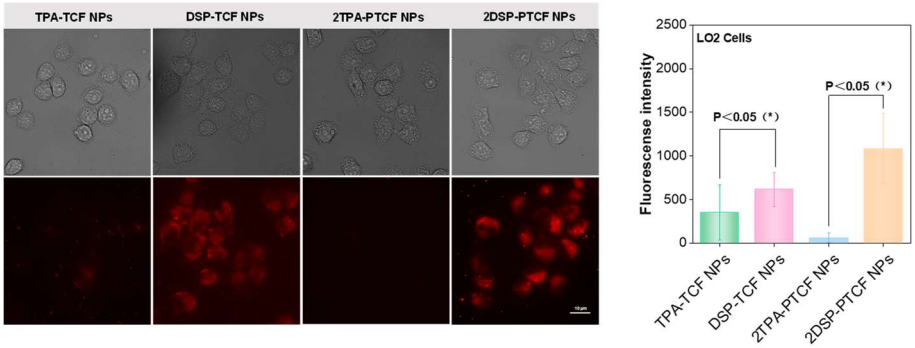

Figure S35. (A) Fluorescence imaging of LO2 cells in the presence of the four NPs (10 μM) after 12 h incubation. (B) Corresponding fluorescence intensity of four NPs in LO2 cells.

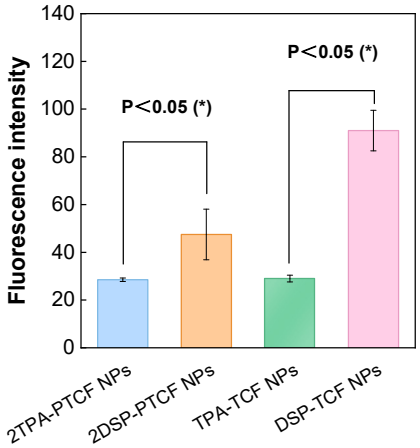

Figure S36. Fluorescence intensity of 4T1 cells treated with the four NPs after solubilization (n = 3). The 4T1 cells were incubated for 12 h after treatment with four NPs.

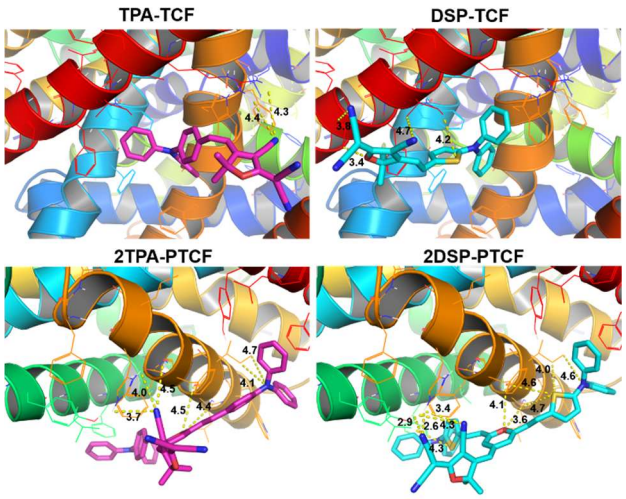

Figure S37. The molecular docking of four compounds to transmembrane transport proteins (PDB: 3USI).

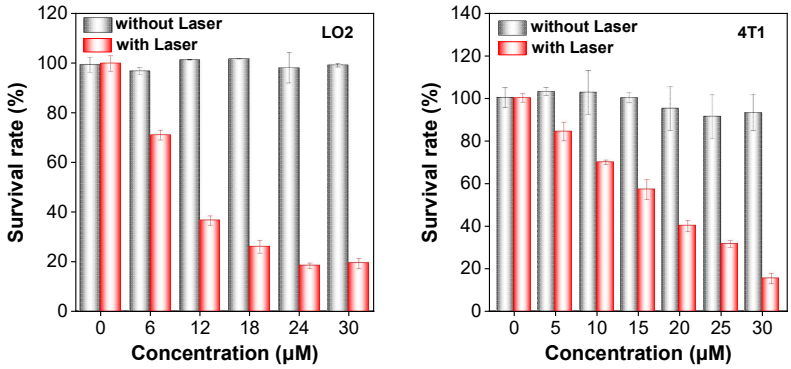

Figure S38. In vitro cytotoxicity assay of 2DSP-PTCF NPs toward (A) LO2 and (B) 4T1 cells.

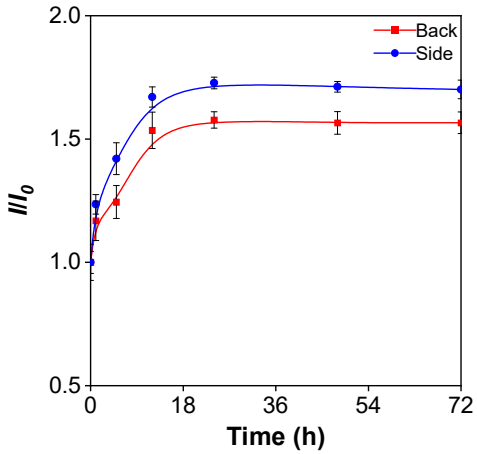

Figure S39. Corresponding fluorescence signals of the tumor in Fig. 4B after *i.v.* injection of 2DSP-PTCF NPs with irradiation at various time points (0, 1, 5, 12, 24, 48, and 72 h).

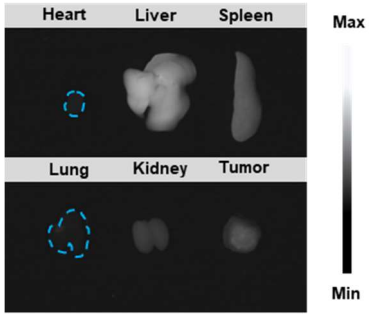

Figure S40. E_x vivo fluorescence imaging of major organs and tumors in mice after *i.v.* injection 72 h of 2DSP-PTCF NPs (400 μM, 150 μL).

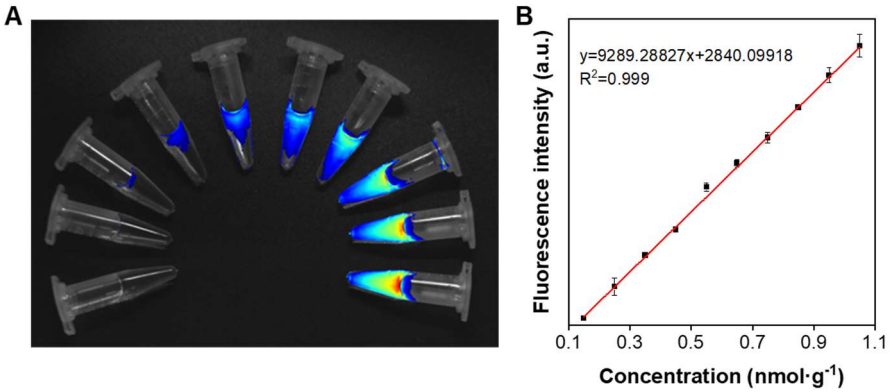

Figure S41. (A) The fluorescence images of 2DSP-PTCF NPs at different concentrations. (B) Fitted calibration curve of FL intensity versus concentration of 2DSP-PTCF NPs.

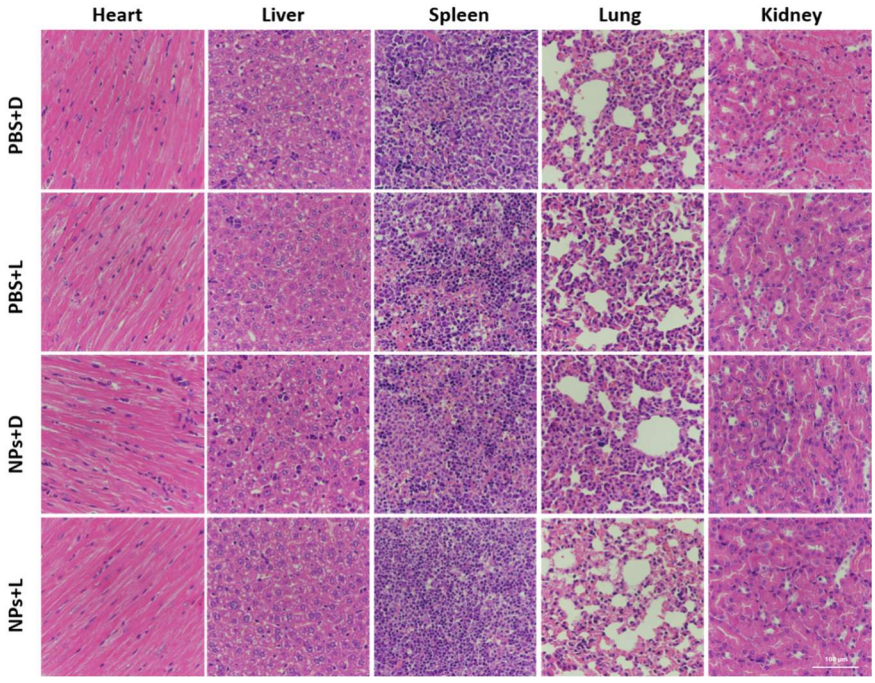

Figure S42. Histological H&E staining of major organs (heart, liver, spleen, lung, kidney) of mice in different groups.

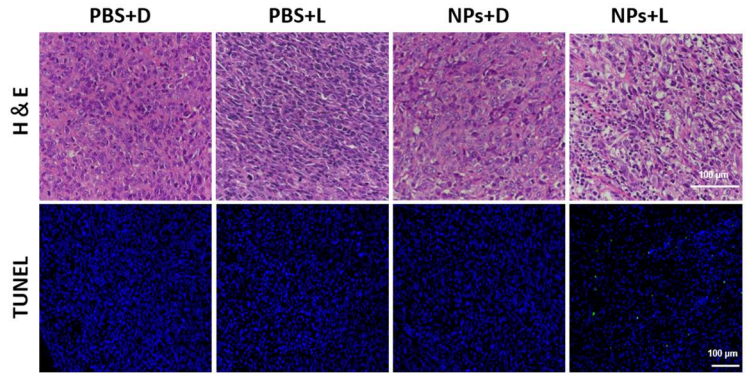

Figure S43. H&E, TUNEL staining analysis of tumor tissues after different treatments.

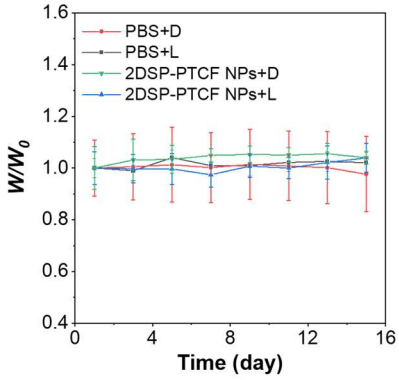

Figure S44. The weight changes of mice within 15 days of different treatments (n=4).

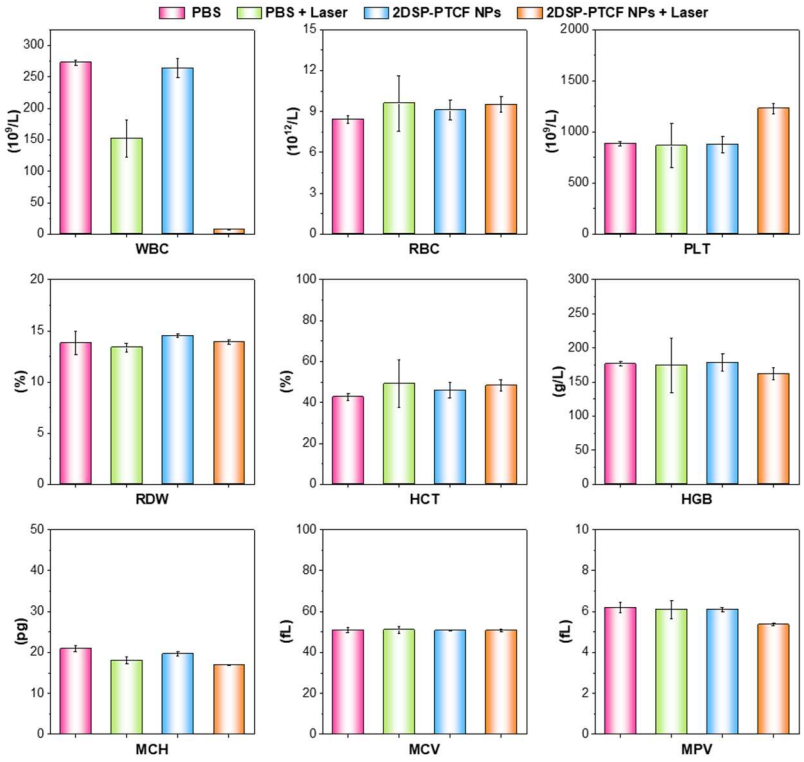

Figure S45. Blood routine assays of the healthy mice with and without intravenous injection of 2DSP-PTCF NPs, respectively (n = 3 mice for each group).

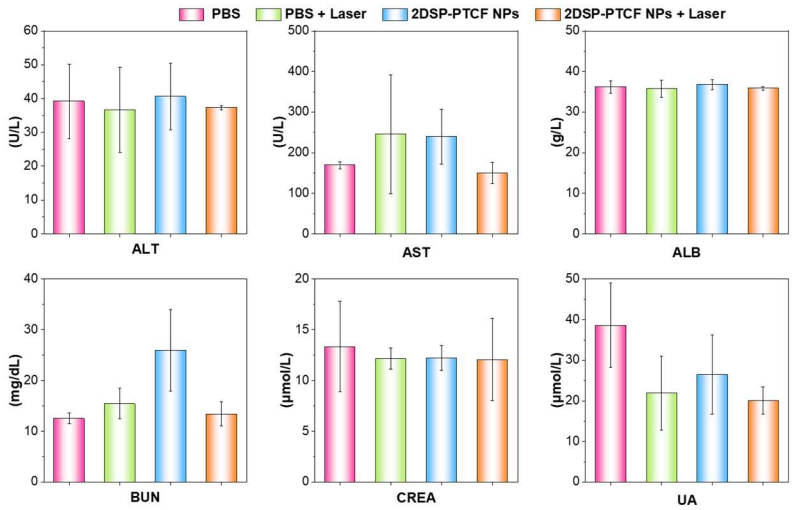

Figure S46. Blood biochemistry test regarding liver and kidney function of the healthy mice with and without intravenous injection of 2DSP-PTCF NPs, respectively (n = 3 mice for each group).

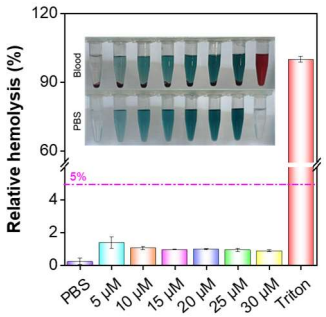

Figure S47. The hemocompatibility of 2DSP-PTCF NPs. Data were presented as mean ± SD derived from n = 3 independent samples per group.

Supplemental References

[1] C. Li, G. Jiang, J. Yu, W. Ji, L. Liu, P. Zhang, J. Du, C. Zhan, J. Wang, B. Z. Tang, Adv. Mater. **2023**, 35, 2208229.

[2] A. Kurutos, Y. Shindo, Y. Hiruta, K. Oka, D. Citterio, Dyes and Pigments, **2022**, 204, 110424.

[3] X. Ran, P. Chen, Y. Liu, L. Shi, X. Chen, Y. Liu, H. Zhang, L. Zhang, K. Li, X. Yu, Adv. Mater. **2023**, 35, 2210179.